

# **Ni-MOF/rGO Composites for Methanol Oxidation in Direct Methanol Fuel Cell**



**Name: Neelam Zaman**

**Reg. No: 00000173019**

A thesis submitted in partial fulfillment of the requirements

For the degree of **Master of Science**

In

**Chemistry**

**Supervised by: Dr. Tayyaba Noor**

**Co-supervised by: Dr. Habib Nasir**

Department of Chemistry

School of Natural Sciences

National University of Sciences and Technology

H-12, Islamabad, Pakistan

**2018**

National University of Sciences & Technology

## MS THESIS WORK

We hereby recommend that the dissertation prepared under our supervision by: NEELAM ZAMAN, Regn No. 00000173019 Titled: Ni-MOF/rGO Composites for Methanol Oxidation in Direct Methanol Fuel Cell be accepted in partial fulfillment of the requirements for the award of **MS** degree.

Examination Committee Members1. Name: DR. MUHAMMAD ARFANSignature: 2. Name: DR. NASEEM IQBALSignature: External Examiner: DR. M. NAVEED ZAFARSignature: Supervisor's Name: DR. TAYYABA NOORSignature: Co-Supervisor's Name: PROF. HABIB NASIRSignature: 
  
 Head of Department

30/11/2018

Date

COUNTERSIGNEDDate: 30/11/2018
  
 Dean/Principal

## THESIS ACCEPTANCE CERTIFICATE

Certified that final copy of MS thesis written by Ms. Neelam Zaman, (Registration No. 00000173019), of School of Natural Sciences has been vetted by undersigned, found complete in all respects as per NUST statutes/regulations, is free of plagiarism, errors, and mistakes and is accepted as partial fulfillment for award of MS/M.Phil degree. It is further certified that necessary amendments as pointed out by GEC members and external examiner of the scholar have also been incorporated in the said thesis.

Signature: Tayyaba

Name of Supervisor: Dr. Tayyaba Noor

Date: 30/11/18

Signature (HoD): M. Afzal

Date: 30/11/18

Signature (Dean/Principal): [Signature]

Date: 30/11/18

*Dedicated to My Parents*

# Acknowledgements

First of all, praise and thanks to merciful Allah Almighty for His blessings and giving me strength and vision which enabled me to complete my MS degree and may the blessings be on Holy Prophet Hazrat Muhammad (PBUH) who is a symbol of guidance.

I would like to pay my deepest thanks and gratitude to my supervisor **Dr. Tayyaba Noor** who gave me guidance and precious time to carry out my research work. Not only she gave me opportunity to be her student but she helped me out of every problem throughout my research work, guided me on every step.

I pay my special thanks to co-supervisor **Dr. Habib Nasir** for taking interest in my research field and for giving expert views and suggestions to make it more productive.

I am thankful to GEC members **Dr. Muhammad Arfan** and **Dr. Naseem Iqbal** for giving valuable constructive suggestions and informative discussions. I am thankful to all the rest of faculty members and staff of SNS for providing a peaceful environment.

I appreciate the facilities provided by SNS, and SCME NUST which enabled me to complete my thesis.

*Neelam Zaman*

# Abstract

The substantial inflation in energy consumption has led to research activities in the development of renewable energy fuel cells. DMFC is an extraordinarily promising energy source because of its easy handling and fuel processing. Direct methanol fuel cells convert chemical energy into electrical energy through methanol oxidation. Research in the preparation of non-noble metal based catalysts for methanol oxidation has been accelerated. During the last decade, the electro-oxidation of methanol at MOFs and their composites with rGO has attracted appreciable attention in DMFC. Here, we report the electrochemical activity of Ni-MOF and its composites with rGO for methanol oxidation. The prepared Ni-based MOFs and their composites with rGO were synthesized via a hydrothermal method. The prepared catalytic material was characterized through scanning electron microscopy, electron dispersive spectroscopy, X-ray diffraction, and FTIR for testing their structural and morphological changes. The electrocatalytic activity and stability of the prepared catalyst were investigated for methanol oxidation through cyclic voltammetry, electron impedance spectroscopy, and chronoamperometry in an alkaline medium. The electrochemical parameters were calculated by a glassy carbon electrode modified with Ni-MOF and their composites, illustrating the effect of rGO on the oxidation of methanol. Among all the composites, 5wt% rGO/Ni-MOF illustrates an excellent peak current density of  $275.85 \text{ mA/cm}^2$  at a lower scan rate of  $50 \text{ mV/s}$  and stability up to 60%. The increased electrochemical activity and considerable stability are associated with the combined effect of rGO with MOFs for methanol oxidation.

# Table of Contents

Abstract.....	v
List of Tables .....	viii
List of Abbreviation:.....	ix
List of Figures:.....	x
Chapter 1: Introduction .....	1
1.1. Fuel cells and their types .....	1
1.1.1. Alkaline fuel cell.....	2
1.1.2. Phosphoric acid fuel cell.....	3
1.1.3. Polymer electrolyte membrane fuel cell .....	3
1.1.4. Solid oxide fuel cell .....	4
1.1.5. Molten carbonate fuel cell .....	5
1.1.6. Microbial fuel cell.....	6
1.1.7. Direct methanol fuel cell.....	7
1.2. History of MOFs .....	8
1.3. Introduction of porous solids.....	8
1.4. Metal organic framework .....	9
1.5. Synthetic routes of MOFs .....	10
1.5.1. Solvothermal synthesis.....	10
1.5.2. Microwave synthesis.....	10
1.5.3. Mechanochemical synthesis.....	10
1.5.4. Electrochemical synthesis .....	11
1.5.5. Sonochemical synthesis.....	11
1.5.6. Slow evaporation method.....	11
1.6. Applications of MOFs .....	13
1.6.1. MOFs for sensing application .....	13
1.6.2. Application of MOFs in gas storage.....	13
1.6.3. Application of MOFs in gas separation.....	14
1.6.4. Applications of MOFs in catalysis .....	14
1.6.5. Applications of MOFs in drug delivery.....	15
1.7. Characterization techniques .....	15
1.7.1. X-ray diffraction (XRD).....	15

1.7.2. Fourier transform infrared spectroscopy .....	17
1.7.3. Scanning electron microscopy.....	18
1.7.4. Cyclic voltammetry .....	20
1.7.5. Electron impedance spectroscopy.....	22
1.8. Experimental techniques .....	23
1.9. Research objectives:.....	24
Chapter 2: Literature review .....	25
Chapter 3: Experimentation .....	31
3.1. Synthesis of Ni-MOF .....	31
3.2. Synthesis of GO .....	31
3.3. Synthesis of rGO .....	32
3.4. Synthesis of Ni-MOF @rGO composites .....	32
3.5. Electrochemical setup .....	33
3.6. Preparation of working electrode;.....	34
Chapter 4: Results and discussion.....	35
4.1. Characterization .....	35
4.1.1 X-Ray diffraction .....	35
4.1.2 Scanning electron microscopy analysis .....	36
4.1.3 Energy dispersive X-ray spectroscopy.....	38
4.1.4 Fourier transform infrared analysis .....	39
4.2. Electrochemical analysis .....	40
4.2.1 Cyclic voltammetry .....	40
4.2.2 Electron impedance spectroscopy.....	45
4.3. Chronoamperometry.....	48
4.4. Tafel studies .....	49
CHAPTER 5 .....	52
5.1. Conclusions .....	52
5.2. Future recommendations .....	52
References.....	54



# List of Tables

Table 3.1. Reaction steps in preparation of Ni MOF and its composites with rGO .....	33
Table 4.1. Comparison of scan rates, current densities and voltages with Ni MOF and its composites (1wt%, 2wt%, 3wt%, 4wt%, 5wt %) rGO/Ni MOF with reported catalysts.....	51

# List of Abbreviation

AC	Alternating current
BDC	Benzene dicarboxylate
CA	Chronoamperometry
CNT	Carbon nanotubes
CV	Cyclic voltammetry
DMF	Dimethylformamide
EDS	Electron dispersion spectroscopy
EIS	Electrochemical impedance spectroscopy
FTIR	Fourier transform infrared spectroscopy
GCE	Glassy carbon electrode
GO	Graphene oxide
HER	Hydrogen evolution reaction
HOR	Hydrogen oxidation reaction
MCFC	Molten carbonate fuel cell
MFC	Microbial fuel cell
MOF	Methanol oxidation fuel cell
MOR	Methanol oxidation reaction
NASA	National aeronautics and space administration
NMP	N-Methyl-2-pyrrolidone
ORR	Oxygen reduction reaction
PAFC	Phosphoric acid fuel cell
PEMFC	Polymer electrolyte membrane fuel cell
RGO	Reduced graphene oxide
SEM	Scanning electron microscopy
SOFC	Soild oxide fuel cell
TA	Trimesic acid
TEA	Triethylamine
XRD	X-ray diffraction
ZIF	Zeolite imidazole framework

# List of Figures

Figure 1.1. Schematic diagram of alkaline fuel cell [10].....	2
Figure 1.2. Schematic Representation of Phosphoric acid fuel cell [10].....	3
Figure 1.3. Graphic of Polymer electrolyte membrane fuel cell[13].....	4
Figure 1.4. Graphics of Solid Oxide Fuel cell[15].....	5
Figure 1.5. Graphics of Molten carbonate Fuel Cell[10].....	6
Figure 1.6. Graphics of Microbial fuel cell [19].....	6
Figure 1.7. Graphics of Direct Methanol Fuel Cell [21].....	7
Figure 1.8. Schematic Diagram of Metal Organic Frame work[34].....	9
Figure 1.9. (a) Common synthesis routes for MOF preparation (b) Percentage summary of MOFs Prepared by Following various synthesis routes [43].....	12
Figure 1.10. Instrumentation and working principle of X-ray Diffraction .....	15
Figure 1.11. Instrumentation and working Principle of FTIR .....	18
Figure 1.12. Basic structure and working principle of SEM .....	19
Figure 1.13. Potentiostat instruments assembly .....	20
Figure 1.14. Typical Cyclic Voltammogram .....	21
Figure 1.15. Nyquist Plot .....	23
Figure 3.1. Potentiostat / Galvanostat for Cyclic Voltammetry.....	34
Figure 3.2. Modified glassy carbon electrode preparation .....	34
Figure 4.1. X-Ray Diffraction of Ni MOF and its Composites with rGO (1wt%, 2wt%, 3wt%, 4wt% and 5 wt%).....	36
Figure 4.2. SEM images of Ni MOF (a), rGO (b) 1wt%rGO/Ni MOF, (c) 2wt% rGO/Ni MOF (d) 3wt%rGO/Ni MOF (e) 4wt% rGO/Ni MOF (f) 5wt%rGO /Ni MOF (g).....	37
Figure 4.3. EDX of prepared Ni MOF and its composites with (1wt%, 2wt%, 3wt%, 4wt%, and 5wt %) rGO/Ni MOF.....	38
Figure 4.4. FTIR of Ni MOF and its composites with (1wt%, 2wt%, 3wt%, 4wt% and 5wt %) rGO/ Ni MOF.....	40
Figure 4.5. Cyclic Voltammogramme of Bare GCE.....	41
Figure 4.6. Cyclic voltammogramme with different concentrations of Ni MOF .....	41

Figure 4.7. Cyclic voltammogram of Ni MOF composites (1wt% rGO/Ni MOF, 2wt% rGO/Ni MOF, 3wt% rGO/Ni MOF, 4wt%rGO/Ni MOF and 5wt%rGO/ Ni MOF).....	42
Figure 4.8. Cyclic voltammogram of Ni MOF composites with 8wt% rGO/Ni MOF .....	43
Figure 4.9. Cyclic Voltammogramme of Ni MOF and its composites with 1wt%, 2wt%, 3wt%, 4wt% and 5wt% rGO at different scan rates (50mv/s, 100mv/s, 150mv/s, and 200mv/s) in 1 M NaOH and 3 M methanol.....	45
Figure 4.10. Nyquist Plot of bare glassy carbon electrode in 1M NaOH and 3 M methanol.....	46
Figure 4.11. Nyquist Plots of Ni MOF at various concentrations in 1M NaOH and 3M methanol.....	46
Figure 4.12. Nyquist plots of Bare GCE , Ni MOF and its composites 1wt%rGO/ Ni MOF, 2wt% rGO/Ni MOF, 3wt% rGO/Ni MOF, 4wt% rGO/Ni MOF and 5wt% rGO/ Ni MOF in conc.2mg at 50mv/s .....	47
Figure 4.13. Plots of square of scan root vs. peak current density for Ni MOF and its composites ( 1wt%, 2wt%, 3wt%, 4wt%, 5wt% ) rGO/Ni MOF .....	48
Figure 4.14. Chronoamperometry curves for Ni MOF and its composites (1wt%, 2wt%, 3wt%, 4wt%, 5wt %) rGO /Ni MOF in 3M methanol and 1 M NaOH.....	49
Figure 4.15. Tafel plots for Ni MOF and their composites with rGO in 3M methanol and 1 M NaOH.....	50

# Chapter 1

## Introduction

Utilization and production of energy is the indication of industrial progress and growth of any country because energy derives everything and approximately 85% of our energy commitment we rely on fossil fuels [1]. But recently energy resources such as fossil fuels deplete rapidly due to increasing life standards and growing populations, Moreover industrial civilization, Life style and economic growth of developed countries lean on the energy extraction from gas and oil supplies [2]. According to 2013 survey 86.59% of energy is generated through oil, 23.72% from natural gas and around 30% is generated by coal and the following values decrease rapidly due to increasing demand of energy day by day [3].

As far as in Pakistan the natural gas sector the average short fall is 2 billion cubic feet and estimated short fall in power sector is around 4000 MW and with the passage of time the value raises up to 7000 MW. In Pakistan 140 million Pakistanis suffer over 12-14 hours load shedding and most of the areas have no access to power grids [4].

To cope this increasing shortfall in power sector we need an alternative environment friendly energy resource which is not only full fill our energy demand but also save our environment from harmful gases like ( $\text{CO}_x$ ), ( $\text{NO}_x$ ) and ( $\text{SO}_x$ ) [5].

### **1.1. Fuel cells and their types**

Recently fuel cell is considered to be a promising energy resource in contrast to other alternatives converts chemical energy into electrical energy through a catalytic reaction [6]. It may define as “A device which produces electrical energy from chemical energy of chemical compounds used as fuel through a chemical reaction” [6]

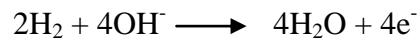
The typical construction of fuel cell consists of cathode and anode, and an electrolyte interceding between cathode and anode [7]. There are various types fuel cells depending upon the type of electrolyte used, power output, electrical efficiency, their operating temperature and application for which they are suitable [8]. Major types of fuel cells are Polymer electrolyte membrane fuel cell (PEMFCs), alkaline fuel cell

(AFCs), Phosphoric acid fuel cell (PAFCs), Solid oxide fuel cells (SOFCs), molten carbonate fuel cell (MCFCs), and direct methanol fuel cells (DMFCs) [9].

### 1.1.1. Alkaline fuel cell

In alkaline fuel cell shown in figure (1.1) power is generated by redox process between oxygen and hydrogen through alkaline solution as electrolyte, and NaOH and KOH solution may use as an electrolyte solution in fuel cell. The overall reactions are

At anode:



At cathode:

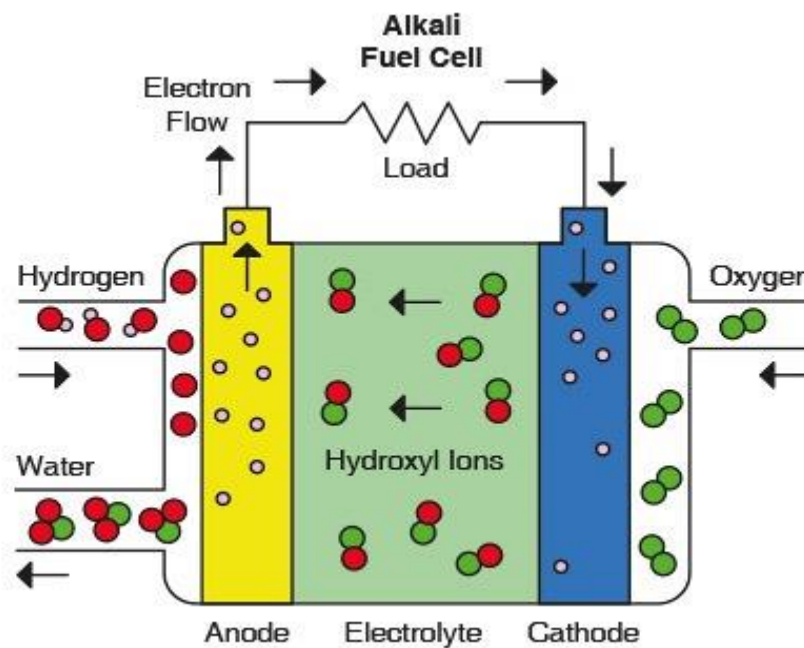
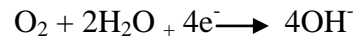


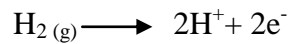
Figure 1.1. Schematic diagram of alkaline fuel cell [10]

It works at 80° and at voltage between 0.5V -0.9V depends on load. Alkaline fuel cells are used in space program and show efficiency more than 60% [11]

### 1.1.2. Phosphoric acid fuel cell

PAFCs shown in figure (1.2) require phosphoric acid as an electrolyte to produce current from an electrochemical reaction and operate at 450° the reaction are:

Reaction at anode:



Reaction at cathode:

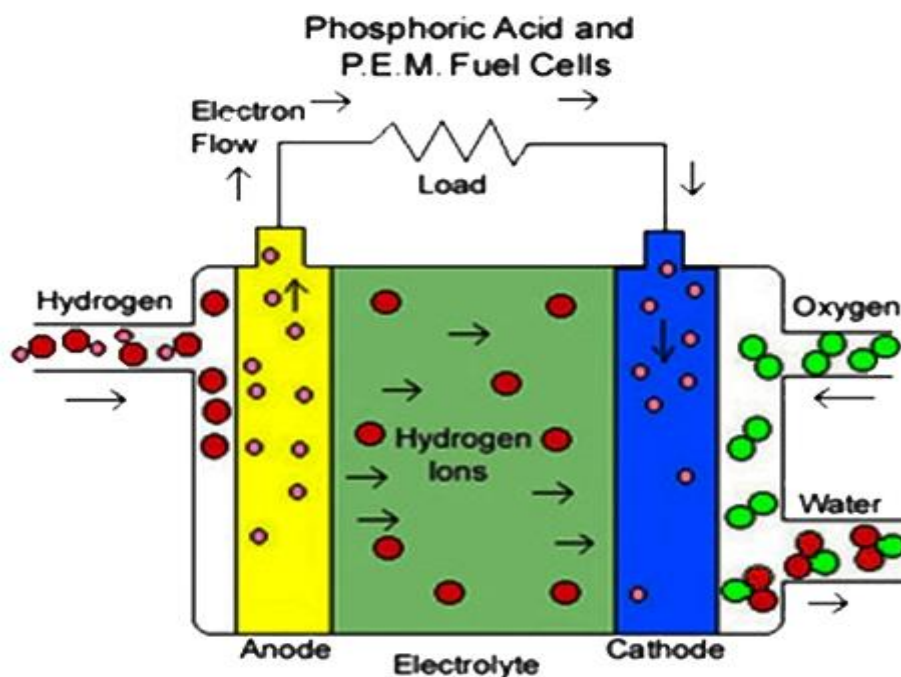
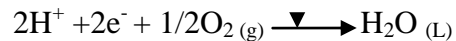


Figure1.2. Schematic representation of phosphoric acid fuel cell [10]

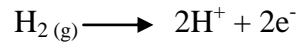
One of the major advantage of (PAFCs) is that uses impure Hydrogen as fuel. First phosphoric acid fuel cell power may install in1970 and now there are about 500 such plants are working in the world [12].

### 1.1.3. Polymer electrolyte membrane fuel cell

A PEMFCs shown in figure (1.3) used polymeric materials as electrolyte. This membrane act as a path way for proton to move from anode to cathode in the cell and

convert chemical energy in to electrical energy. The overall reaction occur in a cell are

Reaction at anode:



Reaction at cathode:

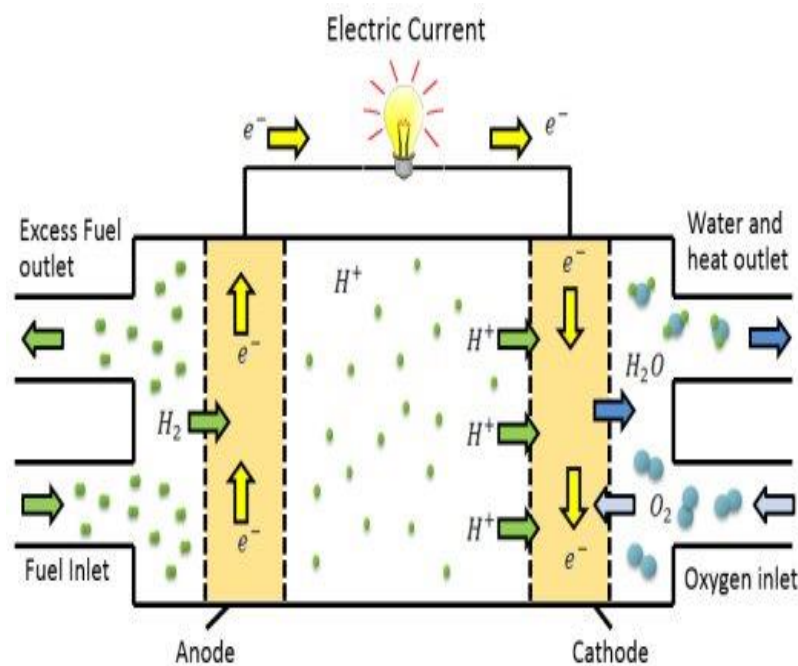
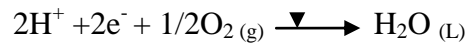


**Figure1.3. Graphic of polymer electrolyte membrane fuel cell [13]**

This fuel cell produces water, Heat and electrical current, main advantages of this cell includes transportation, Portable and in stationary power generation because of its high power density [14].

#### **1.1.4. Solid oxide fuel cell**

Most efficient and environment friendly fuel cell which generates current from renewable fuels i.e. methane, Hydrogen etc and use solid oxide or ceramic as an electrolyte shown in figure (1.4).



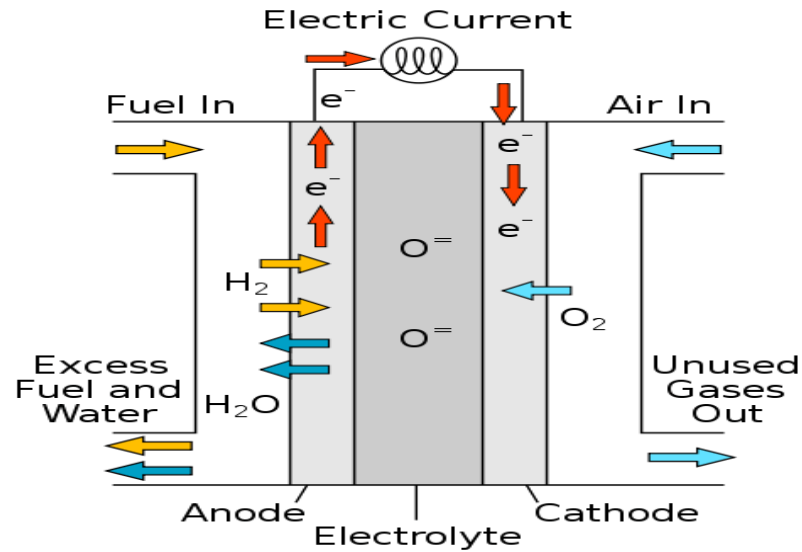


**Figure1.4. Graphics of solid oxide fuel cell [15]**

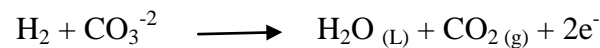
Their main advantage includes its low cost, high efficiency, lesser emission and long term stability. Some problems related to this fuel cell are because of high operational temperature (T) which cause chemical and mechanical stability issues [16].

### 1.1.5. Molten carbonate fuel cell

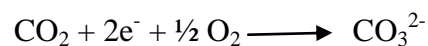
Like other fuel cell working of this fuel cell based on same electrochemical reactions, but with the assistance of carbonate compounds which act as electrolyte shown in figure (1.5).

Overall reactions are

At Anode:



At cathode:



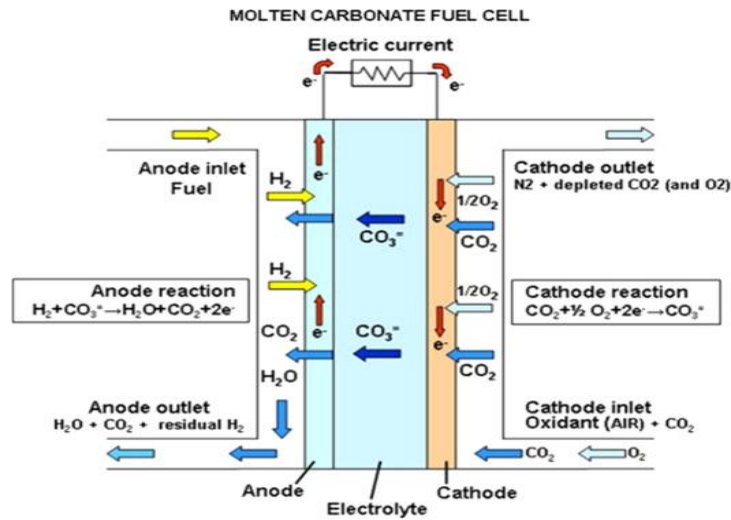


**Figure1.5. Graphics of molten carbonate fuel cell [10]**

MCFCs main applications are in power plants (natural gas and coal based) for industrial [17].

### 1.1.6. Microbial fuel cell

Microbial fuel cells shown in figure (1.6) are biological fuel cell they derive current by using bacteria, their setup is similar as having cathode and anode connected through external wire these bio films are deposited over anode which oxidized the fuel biologically rest of the setup is similar. They only difference lies in the fuel type typically based on organic substance originated from living organism [18].

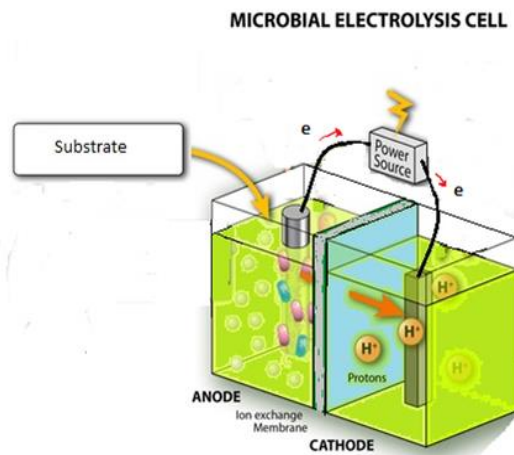


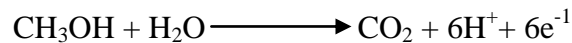
**Figure1.6. Graphics of microbial fuel cell [19]**

### 1.1.7. Direct methanol fuel cell (DMFCs)

DMFC shown in figure (1.7) directly converts the energy of fuel to electrical power this property makes them most efficient and attractive fuel cell among other fuel cell types which are established on conventional hydrogen fuel [20]. Moreover this fuel cell is especially best for transportation applications.

Overall reactions on the surface of electrode and anodes are

At Anode:



At Cathode:

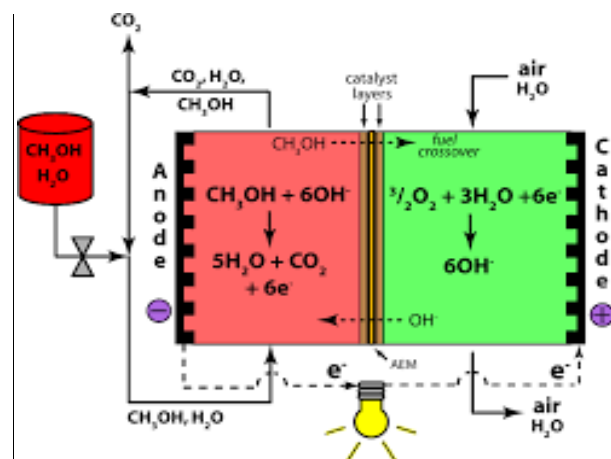
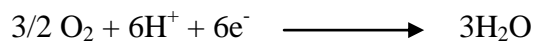


Figure1.7. Graphics of direct methanol fuel cell [21]

Fact that delays the commercialization of this fuel cell is its anodic performance and they need more efficient catalysts for methanol oxidation. Various catalytic materials have been tested based on non noble and noble metals. It is noticed that only platinum shows high current density. Vast research is being done to search for competent catalyst with adequate current density which could be a replacement to the expensive platinum based catalysts [22].

## 1.2. History of MOFs

The ascendant of MOF can be recorded in back 1706 when a pigment “Prussian blue” was manufactured. Its Crystal structure shows cubic network topology in which four and six coordinated Fe (II) , Fe (III) are linked by cyanide ( $\text{CN}^-$ ) ligands. After 273 years this pigment is identified as the initial coordination polymer. Their uniformity regularity and beauty of the crystal inspired MOF chemist to build up materials with complementary structure [23]. In 1990 Robson suggested the instinctive self assembly among four and six coordinated metal nodes and linear organic ligand. The term metal organic framework was first suggested by Yaghi in 1995. The undeniable improvement happened in 1999 when William and Yaghi individually reported two materials HKUST-1 and MOF-5 [24].

Since then the investigation on partly organic and inorganic materials was start off. These hybrid of Organic and inorganic Framework described a new class of porous compound Known as Metal organic Frameworks .Their framework based on metals as connectors and ligand as linkers, Where metal ligand bond can joined the following metals and ligands as a result a crystalline structure is obtained. These following structure has two central characteristics, First one is these have considerable porosity and other one is that have large surface area. For obtaining considerable porosity and surface area the structure of organic ligand (linker) can be wisely adjusted, thus made them assuring candidate for different applications include storage of gases separation of molecules, catalyst and so on [25].The uniqueness of each MOF for a given applications derives from its particular well defined crystalline structure. It is mandatory to maintain porous framework without any alteration over the series of a processes, specifically for functional application the stability is important condition to be fulfilled. Moreover different properties are tuned just by modification of organic linkers; Because of this many reactions which are not possible to done in a solution can be done inside the pores of these frameworks and spectroscopy techniques can be used to monitor this chemical reaction [26].

## 1.3. Introduction of porous solids

In scientific community Porous solids acquired great importance because of their appropriateness as host materials, and host more molecules due to presence of empty voids. On the basis of their pore size they are classified as micro pores and macro

pores. The micro pores have pore size up to 2nm and macro and meso pores have pore size up to 50nm and  $\geq 50\text{nm}$  [27].

The primary characteristics of these substances are porosity, pore size and surface area. Most influential applications of such substances are Filtering, molecular sensing, and storage of small molecules [28]. The most familiar porous materials activated carbon an important organic substance with surface area over  $200\text{m}^2\text{g}^{-1}$ , adsorb different variety of molecules and gases. An exclusive feature of activated carbon are their variation in pore aligning, size, their shape and diameter of the pore varies between a range of values [29]. Zeolites are another significant and very familiar porous material comprises of porous inorganic frameworks. This group of material primarily consists of chalcogen, Al, and Si. About 70 contrasting forms of zeolites are familiar today, which shows high degree of order in their molecules. Meso and nanoporous Zeolites are used in washing machines for the cleanliness of textiles. In comparison of activated carbon zeolites have various applications in gas storage, catalysis and gas separation [30].

#### 1.4. Metal organic framework

A new family of porous solids called porous coordination polymer or metal organic framework (MOFs) [31], Typically MOFs are formed by combining metals and ligands through coordination bond. They are characterized by maximum degree of crystallinity, porosity; high surface area and pore size clearly go beyond that of other porous materials [32]. Researchers have discovered that small alteration to functional groups located on the linkers can greatly enhanced MOFs potential properties For example drug delivery, heterogeneous catalysis, gas storage and separation [33].

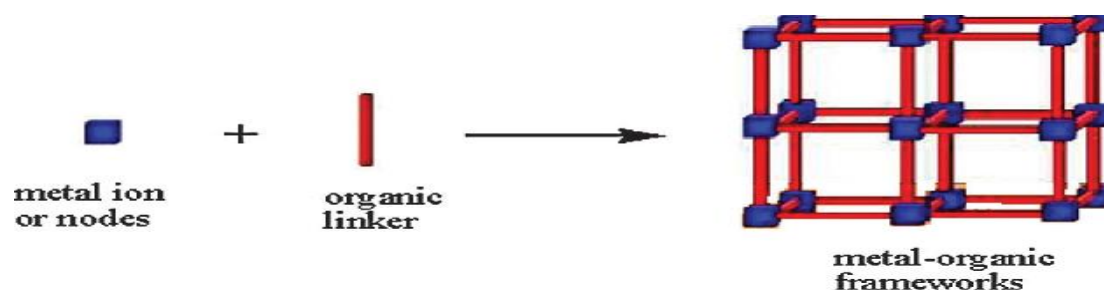


Figure1.8. Schematic diagram of Metal organic frame work [34]

## **1.5. Synthetic routes of MOFs**

There are number of methods which can be used to synthesize MOFs. Including Solvothermal, hydrothermal, sonochemical, microwave heating , mechanochemical and electrochemical synthesis and may more, [35] each synthesis technique can bring about compounds with different size, distribution, particle size and morphologies, normally solvothermal and hydrothermal techniques are used [36].

### **1.5.1. Solvothermal synthesis**

Demand for more prosperous frameworks was confronted preponderant difficulties. Fortunately this technique was established to be a favorable elucidation to these tribulations [37]. This technique is identical to hydrothermal technique of MOF synthesis the particular discrepancy is the precursor solution is generally non aqueous especially high boiling organic solvents usually ethanol, methanol, DMF are commonly utilized. The reaction is carried out in a Teflon lined autoclaves [38].

### **1.5.2. Microwave synthesis**

For the synthesis of MOFs microwave synthesis is an extraordinary quick method, this method greatly shorten the reaction time of MOF synthesis. This attrition in reaction time is because of superheating effect of solvent. This enormous heat production is begin by interaction of microwave with the solvent and give energy to stimulate the synthesis of reaction at location where the boiling nuclei production decreased, Moreover this method allows the production of greater quantity MOFs by regulation of operating conditions of synthesis [39].

### **1.5.3. Mechanochemical synthesis**

MOF synthesis depends on volatile organic solvents, is an issue due to their possibility of environmental contamination, for the reduction of these risk this synthetic method is being established. In this method solvent is not required and chemical reaction is performed by applying mechanical force [40]. Commercially accessible mechanochemistry strategies generally involve ball mills, planetary mills and specifically shakers. In ball mills organic ligand and metal linkers are perfectly mixed by developing friction or crashing the reactants that are located interior to the mills. Shortly this method is preferred over other synthetic methods due to Its lower solvent cost, synthesis time and energy uses of MOF synthesis [35].

#### **1.5.4. Electrochemical synthesis**

Traditionally the ultimate goals of MOF synthesis are to retrieve high quality crystals for structure dissolution. Now at room temperature the big crystal of MOF in huge quantity is possible to create by changing experimental specification such as solvent type, pH, and temperature [41]. In this synthesis technique metal ion is continuously generated by anodic oxidation of metal source. One of the advantages is that there is no need of metal salt, the final product is pure due to absence of anionic residue and synthesis is fast at low temperature and so on [37].

#### **1.5.5. Sonochemical synthesis**

In this technique Homogenous nucleation is bring about by Ultrasonic radiations. These radiations frequency range up to (20 KHz-10MHz) induces physical and chemical changes by development, growth and spontaneous disruption of bubbles in a solvent [42]. This technique incredibly reduced crystal formation time; smaller crystals are yielded in 30 min without bringing significant change in the properties of the crystals formed[36]. MOF-5 crystals (up to 5-25 $\mu$ m) were acquired in 30 min by this method and NMP is used as solvent [35].

#### **1.5.6. Slow evaporation method**

For MOFs synthesis one of the typically used traditional methods is slow evaporation method which required no energy supply for evaporation of solution, but its major drawback is it require more time [37].

Metal salt and linker are mixed in a liquid and then at room temperature the solution is concentrated. For quicker evaporation and better solubility of reagent, usually required more than one and low boiling solvents [39].

(a)

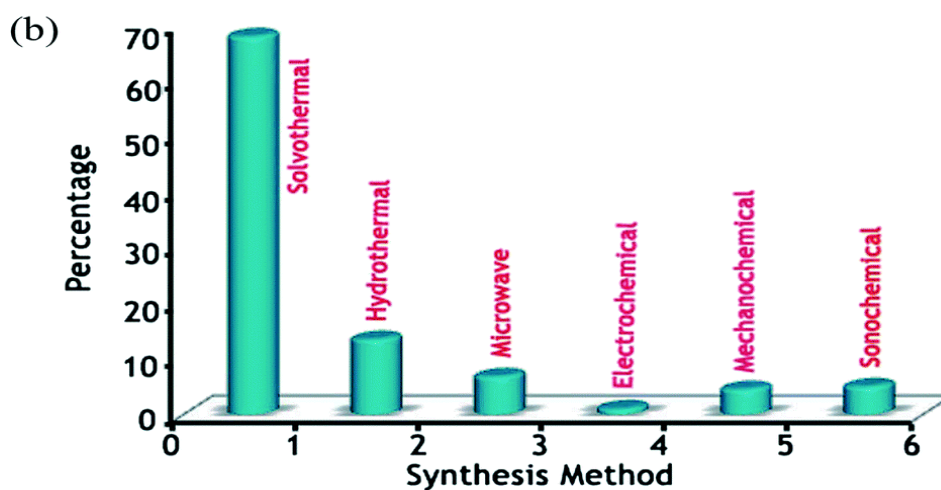
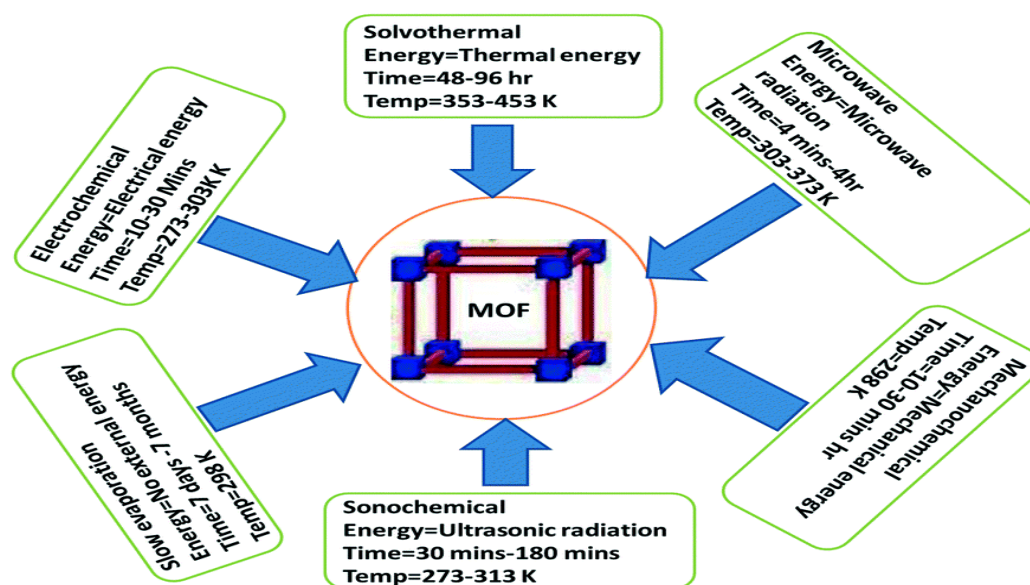


Figure1.9. (a) Common synthesis routes for MOF preparation (b) Percentage summary of MOFs prepared by following various synthesis routes [3,4]



## **1.6. Applications of MOFs**

MOFs were acknowledged to have highly abundant topologies and variety of crystalline structures and have been identified as a material with multiple numbers of functionality. It reveals versatility and admirable properties such as catalysis, gas separation and storage, and sensing, and so on [44].

### **1.6.1. MOFs for sensing application**

A sensor is used to respond various physical and chemical stimulus (sound, pressure, Chemical vapor etc) and conduct resulting impulsions. In MOFs based sensors the MOFs reciprocate extraneous stimulation by manifesting diversity in structure and properties. The structural changes was observed in MOF-5, volume of framework vary with external temperature [37]. MOFs can be examined as magnificent solid-state Fluorescent material as they have structural uniformity and particular environment for the chromospheres in crystalline form. Metal ion such as lanthanide generally utilized for the construction of fluorescent MOFs by reason of their electronic transition with photon emission from d to f shell. As described before MOFs have structural diversity, Flexibility, High surface area, tunable porosity, that make them prominent prospect for sensing application [45].

### **1.6.2. Application of MOFs in gas storage**

In Human society gas storage and separation are firmly associated to different aspects, such as environmental stability, energy regulation and industrial manufacturing. Especially separations of harmful gases such as Ammonia, carbon mono oxide are essential for pollution control and for the preparation of industrial chemicals [46].

MOFs are developing class of Porous crystalline solids and are broadly considered as favorable innovative adsorbent for gas storage and separation because of their particular structural appearance, large surface area, and tunable pore size, have experience viable attention in gas storage [47].

Hydrogen gas is considered to be subsequent fuel by the reasons of substantial heat of adsorption in contrast to gasoline, post combustion non polluting product (primarily water). Although its transportation and storage commenced economic, safety challenges. Recently MOFs materials have fascinated considerable attention due to their simple and productive synthesis, large pore volume, immense storage capacity and permanent porosity [48].

### **1.6.3. Application of MOFs in gas separation**

Separation of gases based on adsorbent pore size/shape and adsorption sites binding affinity [49]. The gas separation can be accomplished by differentiating the size, shape coordination ability, polarities, and polarizabilities of adsorbate molecule. There for separation mechanism can be classified as kinetic, molecular sieving conformation and Thermodynamic separation [50].

In industrial processes gas separation is the most captious challenge, For this purposes MOFs membranes are potential applicants [51], Moreover Micro porous MOFs retains particular premises as membranes for liquid and gas separation, enormous numbers of MOFs have been prepared, but the most stable and focused membranes for gas separation are ZIF membranes, following membranes consist of metal ions such as copper, zinc or cobalt etc bridged by imidazolate or imidazole linkers. In contrast to Zeolites it holds more topological structures, porosity and coordination influences. These membranes illustrate better properties for separation of gases, unavailable for other polymers or inorganic micro pores membranes [52].

### **1.6.4. Applications of MOFs in catalysis**

MOFs share certain characteristics with zeolites such as Chirality, tunable pore size and ordered arrangement of metal ion and organic ligand that make them fascinating for catalysis.

MOFs application in catalysis are determined on the basis of successfully developed synthetic principles, they include catalyst encapsulation in framework, stabilization of catalytically functioning nanosized particles, heterogenization of corresponding catalysis, post synthesis insertion of catalytic metal site and alliance of catalysis with chemical separation [53].

Mostly MOFs catalytic activity relies on metal of the framework, However organic linker can cooperate as well, and perhaps linker's shape and functionality are catalytically active. As a matter of choice linker's may also used as scaffold to which distinct catalytic complexes be able to be confines [54].

In precise, the hybrid (inorganic –organic) nature and nanoporosity of these structures implement numerous opportunities to construct more than one catalytic site inside the pore [44].

### 1.6.5. Applications of MOFs in drug delivery

Novel bioactive compounds synthesis of lower aqueous solubility and high molecular weight with therapeutic action turn out to be more complicated. Moreover their commercialization procedure is very time consuming, so for the better activity of these familiar molecules needs a carrier system, these carrier systems normally increases efficiency and stability of the drugs and moreover reduced their harmful effects [55].

Recently MOFs were introduced as new disciplined delivery systems. These structures have large surface area, prevailing porosity and allow modulation of pore sizes [56].

In MOFs MIL-88, MIL-89 and MIL-53 offer countless prospects to accomplish satisfactory controlled liberation of diversified pharmacological molecules [57].

## 1.7. Characterization techniques

### 1.7.1. X-ray diffraction

XRD a technique employed for the study of crystal structure of the solid materials. Other parameters such as crystal size, atomic spacing, and dimensions of the unit cell and purity of the sample can also be prevailed from XRD [58].

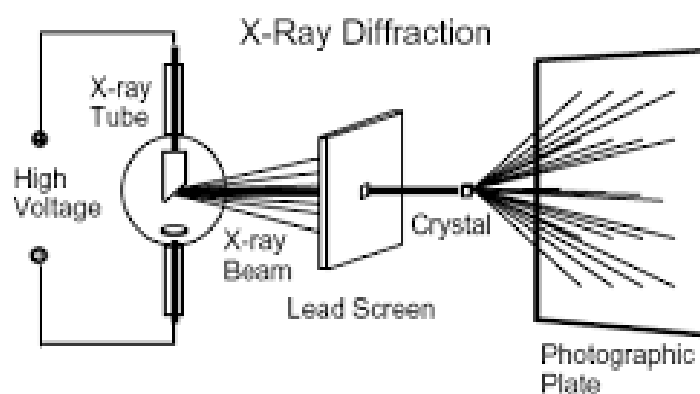


**Figure1.10. Instrumentation and working principle of X-ray diffraction**

By cathode ray tube these rays are generated, filtered to produce the radiations of single wavelength (monochromatic) and collimated to focus and then directed in the direction of sample Figure (1.10)

### **Bragg's law**

In 1913 W.L Bragg explain reflected X-ray patterns, that's law relates interlayer spacing, angle and X-ray wavelength

By the interaction of incident X-rays with the prepared crystalline substance results in constructive interference. When conditions fulfilled, Bragg's law

$$n \lambda = 2d \sin \theta$$

**n**= an integer showing number of layers

$\lambda$  = wave length

**d** = interlayer spacing

$\theta$ = diffraction angle

This law interrelates the wavelength of the radiations (X-ray) to the diffraction angle and interlayer distance in a crystalline substance [59].

### **Debye Scherer equation**

By employing Debye Scherer equation the particle size can also be calculated [60]

$$D = K \lambda / \beta \cos \theta$$

Where

$\lambda$  = wavelength

$\theta$  = diffraction angle

**D** = crystallite mean size (nm)

$\beta$  = Full width at half maximum (FWHM)

**k** = Shape factor

## **Applications of XRD**

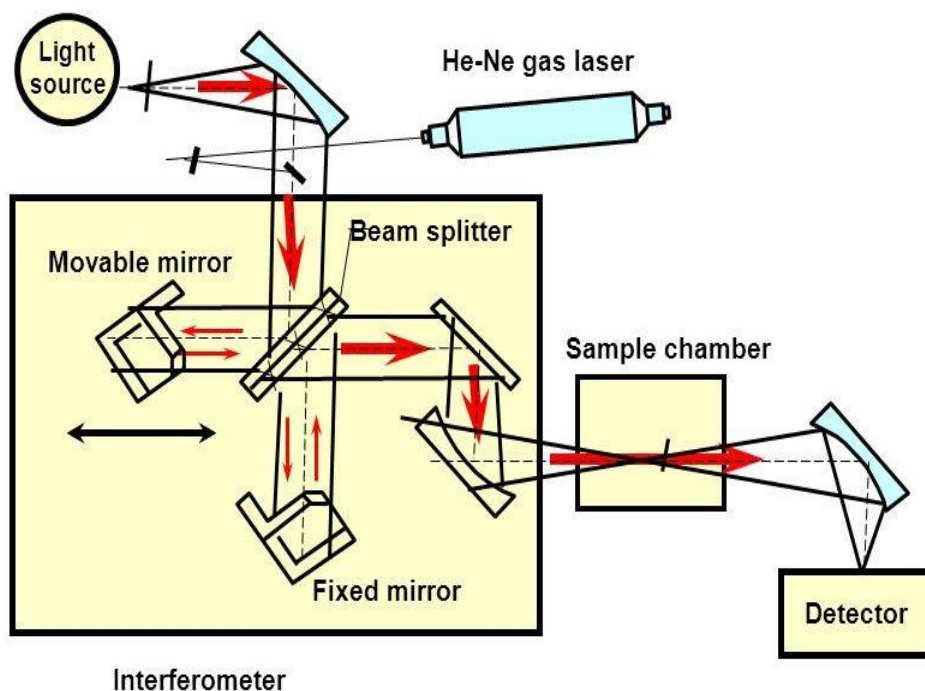
- Distinguish amorphous and crystalline nature of targeted materials
- Measure phase purity
- Identify crystalline structure of unknown materials
- Detect arrangement of atoms in crystalline material
- Calculation of the particle size by Scherer equation

### **1.7.2. Fourier transform infrared spectroscopy**

Infrared spectrum is another significant source for the study of properties (physical and chemical) of the compounds, this technique work superlatively good through association with Fourier transformation. Figure (1.11)

The main principle of this technique is that the disclosure of any compound to infrared rays results in vibration transition of dipole site of those compounds. Molecules are composed of atoms interconnected by chemical bonds; a molecule absorbs IR radiation only when particular absorption stimulates a peculiar change in its dipoles. Consequently a spectrum is established comprises of bands determined by functional groups present in the targeted compound and also displays the complementary emission or absorption, these results assist in the evaluation of the class to which the following compound concerned .i.e. alcoholic, carbonyl compounds etc [61].

The basic principle and basic structure is demonstrated as;



22

**Figure 1.11. Instrumentation and working principle of FTIR**

### **1.7.3. Scanning electron microscopy**

A microscope was invented in 1950 by Max Knoll. This technique uses a beam of electrons to develop an image of the targeted compound and bring helpful information about composition, crystalline structure, and orientation. SEM utilizes a broad range of magnification and provides images of high resolution. The magnification range is from 20x to 30,000x. Porosity, shape, and particle size can be determined by this technique.

#### **Instrumentation and working of the SEM**

The basic components include the electron gun, electron lens, scanning system, sample stage, detectors, and electronic and display control. In scanning electron microscopy, the electron gun generates electrons and stimulates them to energies in the range of 1-40 keV. The basic purpose of the electron lenses in a microscope is to establish an electron probe on the targeted specimen. The electron gun is of two types: thermionic and field emission. In field emission, a strong magnetic field dislodges electrons from a magnetic tip, which comprises two anodes and is used for the generation of an electric field.

2kV voltage is applied as a result electrons go ahead from the tip and other anode stimulate them into microscope. Beam is focused by the combination of following anodes. Then by condenser lens the beam is concentrated for the formation of a probe, after concentrating this beam is reached through aperture which eliminates electrons. If there is any divergence in the beam stigmators amended the beam and concentrate on to the sample. Deflector coils move the beam over the sample and then signal is collected continuously to get the image on monitor.

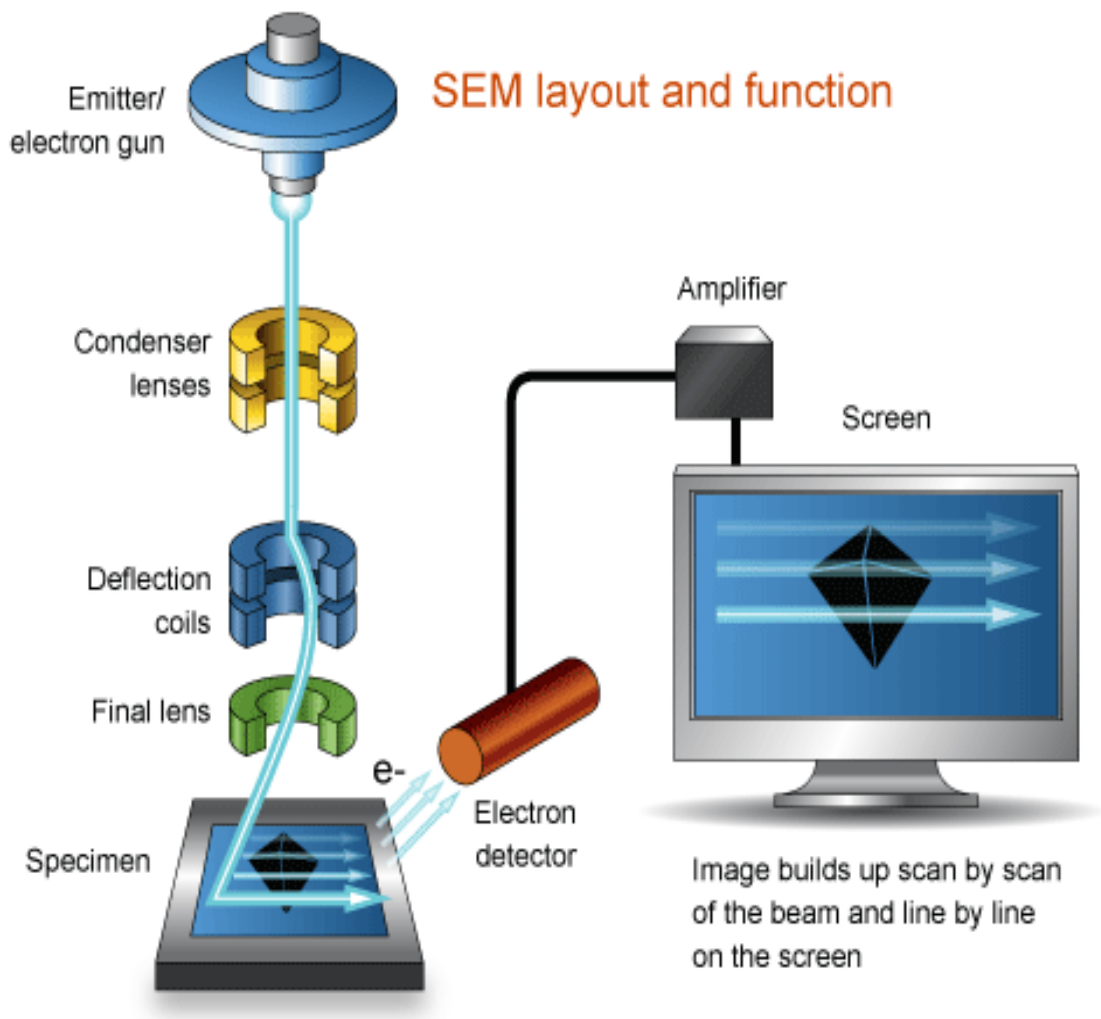


**Figure1.12. Basic structure and working principle of SEM**

SEM works very quickly it accomplished SEI, EDS and BSE analysis in approximately five minutes. It is easy to operate and user friendly. It gives us topographical, compositional and morphological information. Moreover it can also find out the crystalline structure of the sample [62].

## Applications of SEM

In scientific field SEM has number of applications

- Analysis and detection of surface fracture
- For identification of crystalline structure and extraneous morphology
- Reveal alterations in chemical compositions
- Best tool for examining alloys and steel topographical features

### 1.7.4. Cyclic voltammetry

Cyclic voltammetry an electro analytical technique, used for reviewing reactions on electrodes. It provides qualitative information about rate constant, diffusion coefficient and redox potential. It comprises of electro analytical cell with three electrodes (working, Reference and counter) and solution which contains electro analytically active specie.

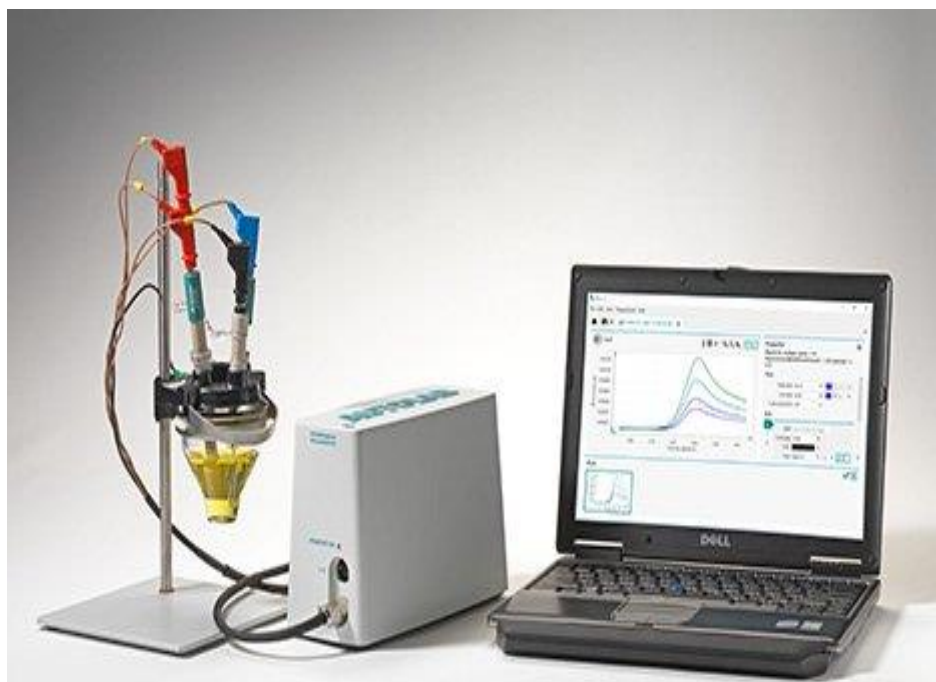


**Figure1.13.Potentiostate instruments assembly**

Working electrode (glassy carbon or platinum electrode) where the reaction of our concern occur, Working electrodes are of distinct shape and forms like rotating disc, rotating ring disc, ultra microelectrode and dropping mercury electrodes. Another



electrode in electrochemical cell with stable potential in contrast to other electrode is reference electrode should maintain the reversible half reaction. There are different type of reference electrodes are available such as copper (II) sulphate, Ag/AgCl, and SCE. Its role is to control and measure the potential of working electrode. The auxiliary electrode needed for balancing the current on working electrode, carbon, platinum and gold are the material for counter electrode.

In CV electrolyte and solvent determines the potential observed in all along experiment, an electrolyte is added to furnish tolerable conductivity.

Voltammogramme is the manifestation of current verses potential as shown in Figure(1.14) In CV after arrival to the set value of the potential the working electrode potential is stimulated to incline back to initial set value.

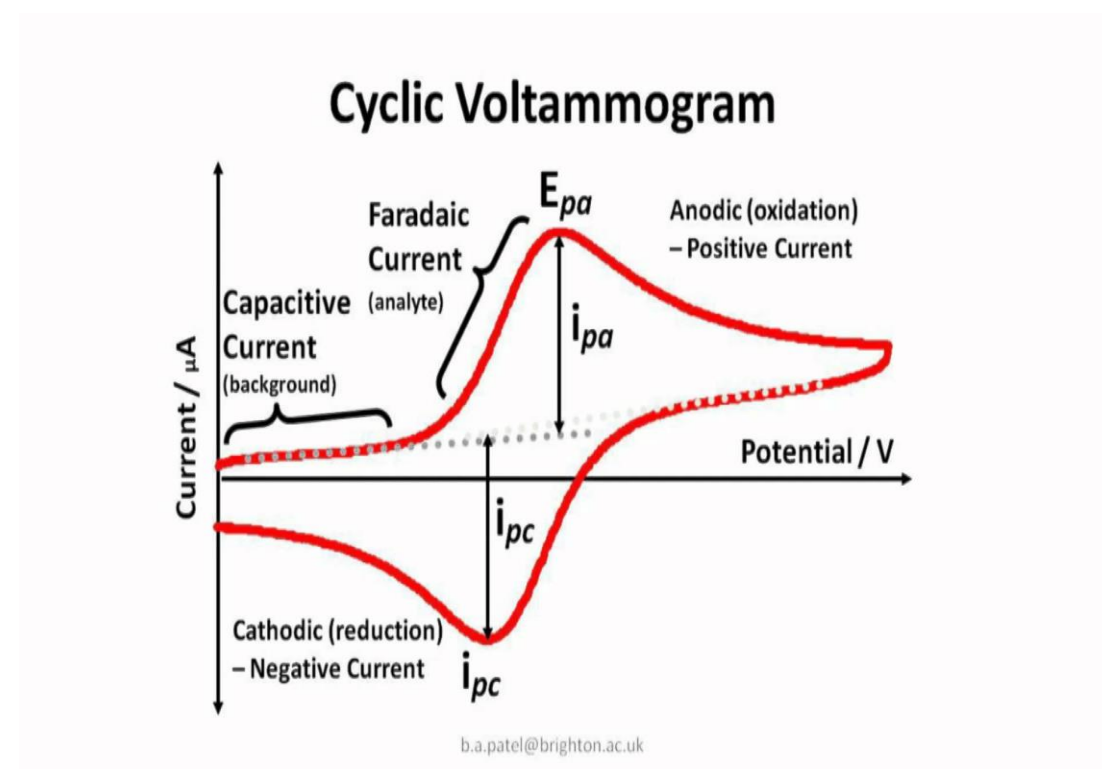


**Figure1.14. Typical Cyclic voltammogram**

Where

$I_p^a$  = Anodic peak current

$I_p^c$  = Cathodic peak current

$E_p^a$  = Anodic peak potential

$E_p^c$  = Cathodic peak potential

CV an electro analytical technique has been used in different field of chemistry to determine redox processes, electrons stoichiometry and electron transfer kinetics, more over concentration of unknown solution can also be resolved by this method [63].

### 1.7.5. Electron impedance spectroscopy

Electron impedance spectroscopy a non destructive analytical technique also known as Dielectric spectroscopy, Measures sample dielectric properties as a function of frequency. Varying frequencies of AC voltage is applied to sample and a plot of impedance change vs. frequency is drawn for analysis. Impedance ( $Z\omega$ ) is specified to overall resistance displayed by system, Moreover on frequency and in complex number it can represented and it is retrieved by an equation

$$Z\omega = V\omega / I\omega = Z_0 \exp(i\Phi) = Z_0 (\cos\Phi + i\sin\Phi)$$

Where

$V\omega$  =voltage depends on frequency

$I\omega$  =current depends on frequency

$\omega$  = angular frequency

And it can measure over vast range of frequency (100 kHz to 10 M Hz.) [64]

EIS data are represented either as nyquist or Bode plot, particularly impedance data proceeds in nyquist plot. A nyquist plot shown in figure (1.15)

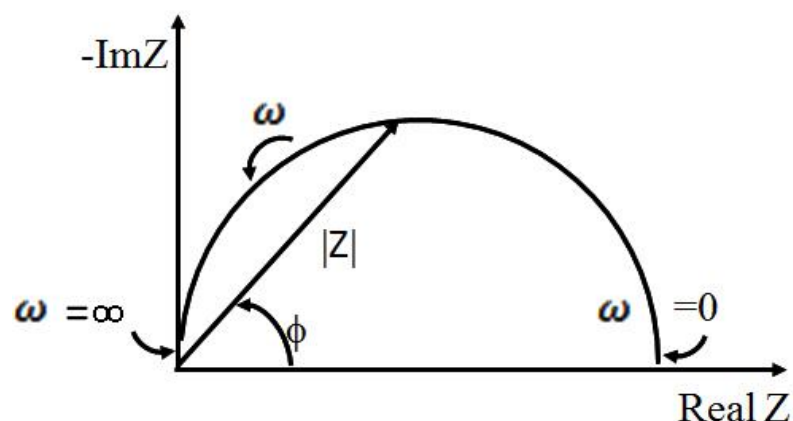


**Figure1.15. Nyquist plot**

CV and EIS setup is similar only we need to operate in galvanized or potentiostat mode

#### **Advantages of EIS**

- Provide comprehensive information of system such as reaction kinetics and electrochemical mechanism.
- Non destructive electrochemical method for interpretation of vast range of substances
- Useful in metallic electrode corrosion study

## **1.8. Experimental techniques**

### **1.8.1. Hydrothermal method**

Hydrothermal synthesis attributes to the crystallization of substances beyond ambient temperature and pressure. The crystallization is executed by establishing temperature difference while heating and then subsequent cooling of the mixture. This technique not only facilitates the processing of homogenous and mono dispersed nano particles but also help in the processing of nano composites and nano hybrid materials. The term Hydrothermal originated from geology.

In 1845 “Karl Emil Von Schafhault” subsided First report on growth of hydrothermally synthesized crystals, He accomplished this experiment in pressure cooker. “Giorgio Spezia” reported macroscopic crystals growth in 1905 [65].

The growth of the crystals executed in an apparatus known as autoclaves, this autoclave must sustain high pressure and temperature for prolonged duration of time. Moreover their material must be corrosion free and inactive toward solvent used. To preclude corrosion of intrinsic cavity of autoclave preservative inserts are used, their shape is similar to autoclave and fit in the intrinsic cavity and they are made up of Gold, copper, titanium, silver, silver and Teflon. The choice of material depends on the temperature of solution used. These sealed autoclaves follow the working principle of pressure cooker. By this synthesis technique a huge number of compounds have been manufactured. Moreover it is applicable in preparing compounds of relatively all classes (carbonates, oxides, silicates etc) [66].

Followings are some advantages of this technique

- Obvious and precise control of size, crystallinity and shape of the product by regulating the specifications such as reaction time, temperature, precursor type and surfactant type.
- Product of metastable, specific phase and intermediate state may be conveniently produced.
- Chemical activity of the reactant significantly enhanced by this method, the materials which cannot be procured by solid state reaction can be synthesized through hydrothermal reaction.

## **1.9. Research objectives**

This research is based on following objectives;

- To prepare GO (graphene oxide) by Hummers' method
- To prepare rGO (reduced graphene oxide) by chemical reduction method
- To prepare Ni-MOF by hydrothermal method.
- To prepare Ni-MOF/rGO composites
- Characterization by FTIR, XRD, SEM, and EDX analysis.
- Electrochemical analysis through cyclic voltammetry and electrochemical impedance spectroscopy, Chronoamperometry.

# Chapter 2

## Literature Review

**Rimsha Mehek *et al.* [2017]** Reported Co-MOF-71 and Co-MOF-71/GO composites. These materials were prepared by hydrothermal method. characterization and electrochemical techniques i.e. XRD, FTIR, XPS, SEM, CV and EIS were used to analyze the catalytic activity in 3 electrode system i.e. working electrode (glassy carbon electrode), Ag /AgCl electrode (reference electrode) in 3M methanol/ 1M KOH and KOH act as supporting electrolyte.

Their appreciable high current density makes it a promising substitute to the other costly electro catalyst in different fuel cell applications. These materials at 0.1V and 50mV/s showed admirable peak current density ( $29.1\text{mA}/\text{cm}^{-2}$ ). The appreciable electro catalytic activity and stability of prepared material for methanol oxidation was associated with the corresponding effect of Co-MOF and graphene oxide [5].

**Adriana Vulcu *et al.* [2016]** Reported that in aqueous solution HKUST-1 is not very stable, But durable HKUST-1 modified electrode were attained by growth of molten solution over various linkers (TA and Mercaptoas). Characterization and electrochemical techniques i.e. XRD, AFM, and cyclic voltammetry were used to analyze the composition and electrochemical properties of prepared materials. The electrochemical nature of HKUST-1 modified electro catalyst (Au-MMA-HKUST and Au-TA-HKUST) were test in three electrode system consisting of modified gold electrode (working electrode), Ag / AgCl (reference electrode) and Pt wire (counter electrode) in 0.5M CH<sub>3</sub>OH/ 0.5 M H<sub>2</sub>SO<sub>4</sub> at potential (0.98V-1.18V) showed current density  $0.2\text{mA}/\text{cm}^2$  [67].

**Jahan Bakhsh Raof *et al.* [2013]** Reported nickel hydroxide nanoparticles, were synthesized in 0.1M NaOH solution by using consecutive potential scanning. Electrochemical activity and characterization of the prepared catalyst was done by cyclic voltammetry and field emission scanning microscopy (FESEM). The catalytic behavior of prepared catalyst was tested in 3 electrode cell i.e. Ag /AgCl (reference

electrode) Pt wire (counter electrodes) and glassy carbon electrode (working electrode). Ni (OH)<sub>2</sub> NPs was applied as electro catalyst for oxidation of methanol on working electrode. These nanoparticles shows activity toward methanol electro oxidation and show current density 15mA/cm<sup>2</sup> at scan rate 30mV/s [68].

**Yan Wang *et al.* [2017]** Reported Ni/Al<sub>2</sub>O<sub>3</sub>-10, Ni/Al<sub>2</sub>O<sub>3</sub>-5, Ni/Al<sub>2</sub>O<sub>3</sub>-2 ordered mesoporous catalyst were synthesized by solvent evaporation induced self- assembly (EISA) method. Characterization and electrochemical analysis was done by XRD, EDS, TEM, N<sub>2</sub> adsorption, chronoamperometry (CA), and cyclic voltammetry (CV). The electrochemical behavior of prepared catalyst were tested in cell comprises of 3 electrodes such as Ag/ AgCl (reference electrode), Pt wire (counter electrode), and working electrode (modified glassy carbon electrode) and a solution (0.1M NaOH and 0.1M CH<sub>3</sub>OH) at scan rate 20mV/s show current density of 7.3mA/cm<sup>2</sup>, 11.1mA/cm<sup>2</sup> and 4.2mA/cm<sup>2</sup> at 0.62V [69].

**Kyung-Won Park *et al.* [2011]** Reported Pt based catalysts (Pt/Ni, Pt/Ru and Pt/Ru/Ni). Prepared by reduction method with NaBH<sub>4</sub> show activation toward oxidation of methanol in 2 M CH<sub>3</sub>OH and H<sub>2</sub>SO<sub>4</sub> at scan rate 50mV/s using 3 electrode system (GCE, Ag/AgCl, Pt wire are working reference and counter electrode). The current densities attained were 3.79mAcm<sup>-2</sup> for Pt-Ru, 2.27mAcm<sup>-2</sup> for Pt-Ni and 5.57mAcm<sup>-2</sup> for Pt-Ru-Ni alloys [70].

**Han-Xuan Zhang *et al.* [2010]** Reported Broad composition range (Pd-Pt/C, Pd/C, and Pt/C) nano catalysts were used for the methanol oxidation in acidic solution. For analyzing electrochemical behavior cyclic voltammetry and chronoamperometry were employed in 0.5M CH<sub>3</sub>OH and 1M NaOH solution using three electrode systems consisting of modified glassy carbon, Pt wire, and Ag/AgCl act as working, counter and reference electrode at a scan rate Pt/C produced current density of 1.9mAcm<sup>-2</sup> at potential value 0.1V with scan rate 5mV/s. Other Pd/C and Pd-Pt/C had also been tested in the same media [71].

**Almir Oliveira Neto *et al.* [2007]** Reported Pt-Ru/C Pt-Sn/C and Pt-Sn-Ru/C electro catalysts were prepared by reduction process using ethylene glycol as a solvent. Characterization and electrochemical study of the prepared catalyst was done by

cyclic voltammetry, EDX and XRD. These materials show activity toward oxidation of methanol in H<sub>2</sub>SO<sub>4</sub> (0.5M) at 20mV/s scan rate. Generate current density at 0.7V (22.5mAcm<sup>-1</sup>, 13mAcm<sup>-1</sup> and 7.5mAcm<sup>-1</sup>) [72].

Pt-Pd alloys nano particles were applied as catalysts for MOR and were tested at 20mv/s scan rate in 0.5M H<sub>2</sub>SO<sub>4</sub> generated 14x10<sup>-14</sup> mAcm<sup>-2</sup> current density at 0.6V.

**Duhong Chen *et al.* [2015]** Reported star like Pt-Cu/rGO nano particles as electrocatalysts for methanol oxidation. The prepared nano particles were characterized by XRD, TEM, XPS and the electro activity and stability were analyzed by cyclic voltammetry and chronoamperometry in three electrode cell (GCE, SCE and Pt sheet act as working, reference and counter electrode) and in 1 M CH<sub>3</sub>OH and 0.5M H<sub>2</sub>SO<sub>4</sub> generated current density 40.2 mA/mg at 50mV/s scan rate [73].

**Jian Ding Qiu *et al.* [2011]** Reported platinum grapheme nano composites for Methanol oxidation. The prepared nano composites were characterized by TEM, XRD, SEM, and, EDX. The electro chemical behavior of prepared composites were observed by cyclic voltammetry in three electrode system (glassy carbon , Ag/AgCl and Pt wire act as working reference and counter electrodes) and in 1M H<sub>2</sub>SO<sub>4</sub> and 2M CH<sub>3</sub>OH solution show 2.53mAcm<sup>-2</sup> current density at scan rate 10mV/s [74].

**Zhibin He *et al.* [2004]** Reported Platinum Rhodium based catalysts were prepared by chemical reduction method. The prepared catalysts were characterized by SEM, TEM, and EDS. The electrochemical behavior of prepared catalysts was analyzed by cyclic voltammetry in three electrode setup in which carbon nanotube electrode act as working electrode and platinum foil and SCE act as counter and reference electrode applied for MOR in 0.5M H<sub>2</sub>SO<sub>4</sub> and 1M CH<sub>3</sub>OH. At 0.7V produced current density 11mAcm<sup>-2</sup> [75].

**T. C. Deivaraj *et al.* [2003]** Reported Pt-Ni nano particles for methanol oxidation. The prepared electro catalysts were characterized by XRD, TEM, XPS and EDX, and their electrocatalytic activity was investigated by cyclic voltammetry in three electrode system nano composites were used for the methanol oxidation in acidic solution. At 0.4V gave current density 550uA at 60mV/s scan rate [76].

**Lei Yang *et al.* [2006]** Reported Pt-Au NPs for oxidation of methanol. These nanoparticles were characterized by TEM and SEM. The electrochemical behavior was investigated by cyclic voltammetry in three electrode system in which graphite electrode act as working electrode, Pt foil and SHE act as counter and reference electrode. At 20mV/s in 0.1M H<sub>2</sub>SO<sub>4</sub> and 1M CH<sub>3</sub>OH gave current density 1.7mAcm<sup>-2</sup> at 0.7V. While in 2007 current density increases up to 10mAcm<sup>-2</sup> at 50mV/s (scan rate) [77].

**D. Macias Ferrer *et al.* [2018]** Reported Pt/rGO and Pt/NC electro catalyst, Have been prepared by wet impregnation method using Ar-H<sub>2</sub> and citric acid as reducing atmosphere. NC and GO were synthesized by nanocasting and modified hummer's method. The prepared catalyst was characterized by SEM and XRD. The electrochemical behavior of Pt/NC and Pt/rGO were checked by cyclic voltammetry in 1M CH<sub>3</sub>OH and 0.5M H<sub>2</sub>SO<sub>4</sub> using three electrode cell consisting of SEC (reference electrode), Pt wire (counter electrode) and Glassy carbon electrode (working electrode) show mass activity 332mA/mg and 335mA/mg at 20mV/s scan rate [78].

**Xiang Li *et al.* [2015]** Reported electro catalysts Pt/COP/CNTs Have been prepared by ethylene glycol reduction method. XRD, TEM and X-ray photoelectron microscopy were used to characterize the fabricated electrode. The electrochemical behavior of Pt/COP/CNTs were investigated by CV and EIS in 1M CH<sub>3</sub>OH containing 1M HClO<sub>4</sub> by using three electrode system consisting of glassy carbon electrode laminated with catalyst act as working electrode, Pt wire and Ag/AgCl saturated with KCl act as counter and reference electrodes show mass activity 1600mA/mg at scan rate 100mV/s for MOR. The stability of electro catalyst was tested by chronoamperometry at 0.6V [79].

**Xiang Li *et al.* [2018]** Reported Novel (Pt/Ni<sub>2</sub>P/CNTs) electro catalyst have been prepared by hydrogen reduction method. Characterization techniques X-ray photoelectron microscopy, Transmission electron microscopy (TEM) and X-ray diffraction (XRD) were used to characterize the prepared catalyst. The electrochemical nature of Pt/Ni<sub>2</sub>P/CNTs was observed in three electrode system by



CV and EIS. The electro catalyst show mass activity 1400mA/mg at scan rate 100mV/s for methanol oxidation reaction [80].

**Yabei Li *et al.* [2015]** Reported Pt/TiSnO<sub>2</sub>-C catalysts have been prepared by solvothermal method. Characterization techniques electron impedance spectroscopy, Transmission electron microscopy, and X-ray diffraction were applied to characterize the assembled electro catalyst. Cyclic voltammetry was used to analyze Catalyst (Pt/TiSnO<sub>2</sub>-C) electrochemical behavior were examined in 0.5 mol/L H<sub>2</sub>SO<sub>4</sub> and 0.5mol/L CH<sub>3</sub>OH by using three electrode system. The catalysts Pt/Ti<sub>(0.7)</sub>Sn<sub>(0.3)</sub>-C, Pt/Ti<sub>(0.9)</sub>Sn<sub>(0.1)</sub>-C, Pt/Ti<sub>(0.8)</sub>Sn<sub>(0.2)</sub>-C, shows mass activity (352.7mA/mg, 459.6Ma/mg and 400mA/mg) at scan rate 10mV/s and 50mV/s. The stability of materials was tested at 0.6V [81].

**Syed Javaid Zaidi *et al.* [2017]** Reported Pt/CeO<sub>2</sub>-MC, Pt/NdO<sub>2</sub>-MC and Pt/PrO<sub>2</sub>-MC catalysts were prepared with 15% Pt only without using Ru. Characterization techniques cyclic voltammetry, EDX, XRD, XPS, SEM, and FT-IR were used to analyze the electrochemical behavior of prepared catalyst in 2M CH<sub>3</sub>OH and 1M H<sub>2</sub>SO<sub>4</sub> solution at 22°C using three electrode cell consisting of saturated calomel electrode, Pt wire and copper electrode act as reference, counter and working electrode. The catalyst Pt/CeO<sub>2</sub>-MC, Pt/NdO<sub>2</sub>-MC and Pt/PrO<sub>2</sub>-MC show current density 47mA/cm<sup>2</sup>, 41mA/cm<sup>2</sup> and 42mA/cm<sup>2</sup> at 25mV/s scan rate [82].

**R.M. Abdel Hameed *et al.* [2016]** Reported Pt-TiO<sub>2</sub>/C and Pt-CeO<sub>2</sub>/C electro catalysts prepared by using intermittent microwave heating method followed by Pt ion chemical reduction. Characterization and electrochemical techniques i.e. EDX analysis, and XRD analysis electrochemical impedance spectroscopy and cyclic voltammetry were used to test the electrochemical behavior of prepared catalyst in 0.1M CH<sub>3</sub>OH and 0.5M H<sub>2</sub>SO<sub>4</sub> solution in three electrode system consisting of Hg/HgSO<sub>4</sub>/ 1.0M H<sub>2</sub>SO<sub>4</sub> (reference electrode), Pt wire (counter electrode) and working electrode was a commercial carbon rod supported the thin film of prepared electro catalyst. The electro catalyst show current density 3.497mA/cm<sup>2</sup> at 167mV and 7.690mA/cm<sup>2</sup> at 814mV with scan rate 50mV/s [83].

**R.S. Amin *et al.* [2012]** Reported an electro catalyst Pt-NiO/C prepared by following two steps such as precipitation and chemical reduction. Characterization and electrochemical techniques (cyclic voltammetry, chronoamperometry EDX analysis, XRD analysis, and TEM analysis) were used to characterize prepared catalyst. The electrochemical behavior of catalyst were analyze in CH<sub>3</sub>OH (0.6M) and H<sub>2</sub>SO<sub>4</sub> (0.5M) solution in three electrode cell consisting of Hg/HgSO<sub>4</sub>/1M HgSO<sub>4</sub> as reference electrode, Pt wire as counter electrode and working electrode was a electro catalyst thin filament supported by carbon rod (commercially available) show current density 13.20mA/cm<sup>2</sup>, 55.82mA/cm<sup>2</sup>, 45.75mA/cm<sup>2</sup> and 16.41mA/cm<sup>2</sup> at scan rate 10mV/s [84].

**X. Tarru *et al.* [2014]** Reported cobalt nickel alloys prepared by selecting adequate conditions Potentiostatically to acquire the desired ratio of Co/Ni. Characterization and electrochemical techniques such as cyclic voltammetry, X-ray florescence and X-ray photo electron spectroscopy were used to characterize the catalyst. Electrochemical behavior of prepared catalyst were analyzed in 0.1M CH<sub>3</sub>OH and 0.1M NaOH solution in three electrode cell such as Co/Ni thin film act as working electrode, Ag/AgCl and Pt wire act as reference and counter electrodes at a scan rate of 20mV/s with different potential window (0.1-0.6V) [85].

**I. Danaee *et al.* [2008]** Reported modified glassy carbon electrodes (GC/NiCu and GC/Ni) were used for the methanol oxidation in alkaline solution. For analyzing electrochemical behavior cyclic voltammetry and chronoamperometry were employed in 0.1M CH<sub>3</sub>OH and 1M NaOH solution using three electrode system consisting of modified glassy carbon, Ag/AgCl and Pt wire act as working, reference and counter electrode [86].

**Markus Kübler *et al.* [2018]** Reported Pd –Ru catalysts for electrochemical studies of methanol oxidation. The prepared catalysts were characterized by XRD, SEM, and TEM, the stability and electrocatalytic behavior were investigated in 0.1M KOH and 0.5M CH<sub>3</sub>OH by chronoamperometry and cyclic voltammetry in three electrode setup (GCE act as working electrode and platinum sputtered plate ,reversible hydrogen electrode act as counter and reference electrode) give current density 38.9 A/g at 20mV/s scan rate [87].

# Chapter 3

## Experimentation

This section constitute of two parts; catalyst synthesis and electrochemical assembly. Following were the chemicals used; Nickel nitrate hexahydrate ( $\text{NiNO}_3 \cdot 6\text{H}_2\text{O}$ ), Benzene dicarboxylic acid (terephthalic acid), N, N-dimethylformamide (DMF), triethylamine (TEA), graphite powder, sodium nitrate ( $\text{NaNO}_3$ ), conc. sulphuric acid ( $\text{H}_2\text{SO}_4$ ), potassium permanganate ( $\text{KMnO}_4$ ), hydrogen peroxide ( $\text{H}_2\text{O}_2$ ), Hydrazine hydrate ( $\text{NH}_2\text{NH}_2 \cdot \text{H}_2\text{O}$ ) and methanol ( $\text{CH}_3\text{OH}$ ). All reagents and chemicals were procured from Sigma-Aldrich with superlative quality guarantee and without farther alteration they were used.

### 3.1. Synthesis of Ni-MOF

Via hydrothermal method Ni based metal organic framework was prepared[5]. 0.45g of 1, 4-benzene di carboxylic acid was dissolved in 100ml of DMF. Afterward few drops of tri ethyl amine (TEA) and 0.61g nickel nitrate hexahydrate were added with continuous stirring, stirred the solution until all the material was completely dissolved and form a homogenous mixture. After that following solution was poured within Teflon lined autoclave and placed it in to heating oven at  $120^\circ\text{C}$  for 24 hours until the green colored crystal of Ni-MOF were developed.

### 3.2. Synthesis of GO

By Hummer method graphene oxide was synthesized[5]. Graphite powder (2g) and sodium nitrate (2g) were dissolved in 50ml  $\text{H}_2\text{SO}_4$ . Solution was stirred for 2 hours in an ice bath. 6g of potassium permanganate was added slowly (pinch by pinch) for keeping the temperature below  $20^\circ\text{C}$ , allowed the solution to stir for two days. 100ml of water was added there was a sudden rise in temperature; to keep the temperature below  $60^\circ\text{C}$  water was added slowly. Dilution of solution was done by adding 200ml of water followed by addition of 10ml hydrogen per oxide and stirred it for 30 mints after the addition of  $\text{H}_2\text{O}_2$  solution turned in to brown yellow. The product was collected and washed in centrifuge by water until pH was maintained in the range of 6.5-7 and dried it under vacuum.

### **3.3. Synthesis of rGO**

Synthesis of rGO was done by dissolving 100mg GO in 100ml of water. For obtaining clear solution this yellowish brown dispersion was sonicated for 2hours. After that 1ml hydrazine hydrate was added. At 100°C the following solution was heated for 24hours under a water cooled condenser in an oil bath. The rGO precipitate out, through filtration the product was isolated and washed with 500ml of water and 500ml of methanol, the washed black solid precipitate were dried at 50 ° C under vacuum[88]

### **3.4. Synthesis of Ni-MOF @rGO composites**

By following the hydrothermal method particular composites were prepared. For the synthesis of Ni-MOF composites with rGO, 0.45g of terephthalic acid was added in to DMF (N, N-dimethyl formamide) and then few drops of triethylamine was added in to the solution. 0.61g of nickel nitrate was added with continued stirring. After that rGO was added with continuous stirring for 2 hours and for further mixing stirred solution was sonicated, poured the solution in to Teflon lined autoclave and heated for 24 hours at 120 ° C. Precipitation color was according to the added rGO quantity. Crystals were washed and collected, dried it under vacuum.

The array of all the steps is given flow chart

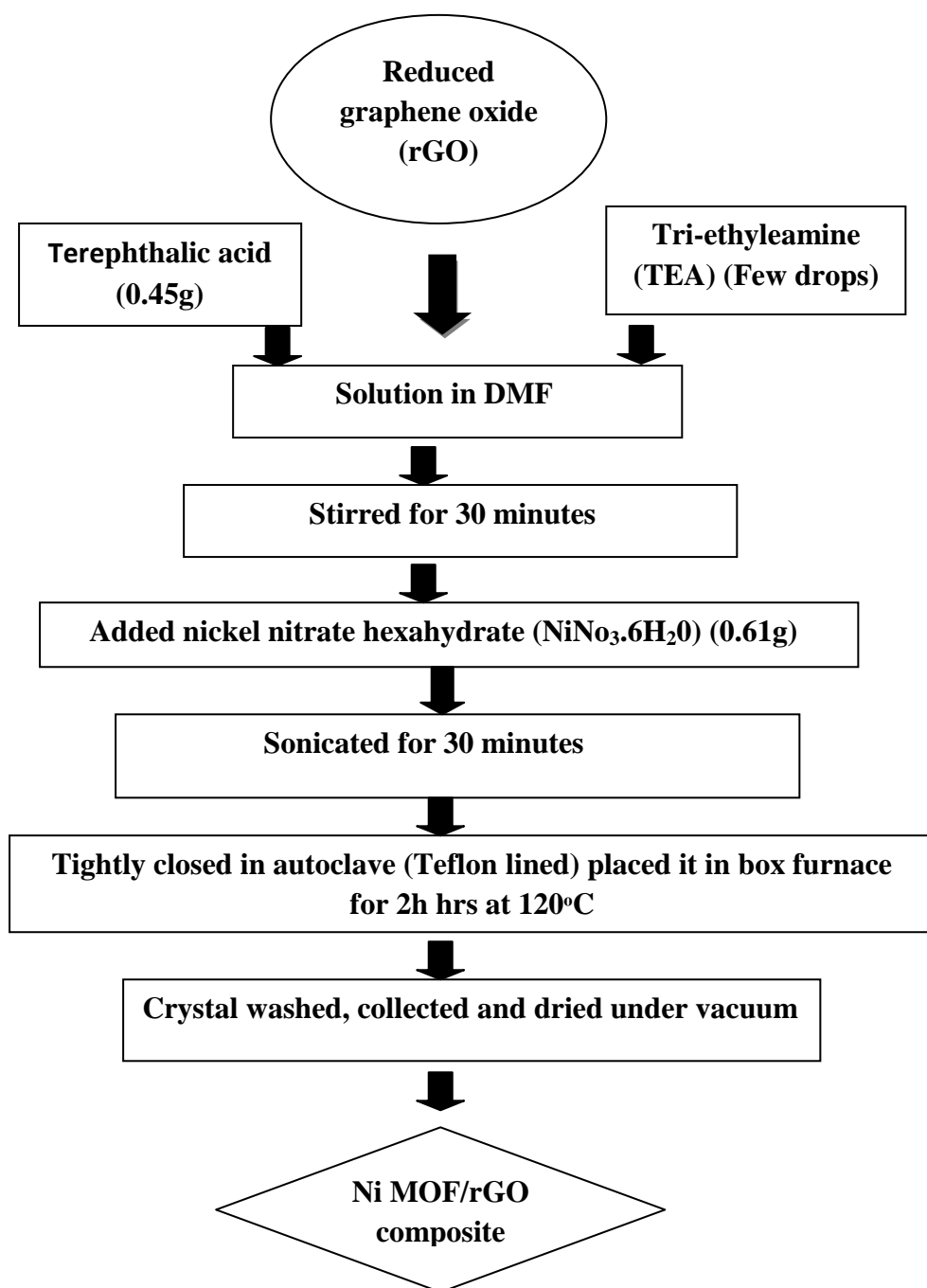


**Table3.1. Reaction steps in preparation of Ni MOF and its composites with rGO**

### **3.5. Electrochemical setup**

Electrochemical activity of prepared catalyst was tested by CV (cyclic voltammetry) in 1M NaOH and 3M methanol. Methanol oxidation reaction was executed in 3 electrode system and GCE (Glassy carbon electrode) act as a working electrode. Firstly the system was run with bare GCE afterward with Modified GCE.



**Figure 3.1. Potentiostat / Galvanostat for cyclic voltammetry**

The EIS (electrochemical impedance spectroscopy) was performed by similar electrode set up in 3 M methanol and 1 M NaOH with bare and modified GEC, and scan rate was 50mV/s. The frequency was set in the range of 10 to 40 KHZ.

### **3.6. Preparation of working electrode**

For the measurement of CV and EIS a particular amount of catalyst i.e. 2 mg, 100ul ethanol and 20ul nafion were mixed thoroughly to make appropriate binding between catalyst material and nafion. After that by using micropipette the mixture was loaded over electrode carefully, before starting up measurement of electrode the surface was dried. All the catalyst was tested at 50mV/s (scan rate) in different concentration and at fixed concentration but Different scan rates.



**Figure3.2. Modified glassy carbon electrode preparation**

# Chapter 4

## Results and Discussion

### 4.1. Characterization

The prepared Ni MOF and its composites crystal structure were confirmed by X-Ray diffractometer (STOE Germany) operated at  $2\theta$  (5-70) with step size 4/s. The as prepared Ni MOF shapes and morphologies were studied by using Scanning electron microscopy (VEG3 TESCAN). Moreover the metal ligand coordination was investigated under Perkins spectrum 100 FT-IR spectrophotometer at wave number ranging from  $400\text{-}4000\text{cm}^{-1}$ .

#### 4.1.1 X-ray diffraction

Ni MOF and its composites with (1wt%, 2wt%, 3wt%, 4wt% and 5wt %) rGO/Ni MOF XRD pattern is shown in figure (4.1).  $2\theta$  value below  $10^\circ$  confirms the successful preparation of Ni MOF and  $2\theta$  at  $44.7^\circ$  corresponds to nano particles of nickel, broad peak at  $25^\circ$  corresponds to rGO give a hint of poor ordering of graphene along their staking direction, Moreover the relative intensity of  $2\theta$  at  $25^\circ$  in all composites shows the rGO concentration increases and these following peaks attributes to large interspacing in between rGO layers and successful incorporation of Ni MOF. The particular purpose of rGO adding in Ni based MOFs is to enhance their surface area and conductivity [89-91].

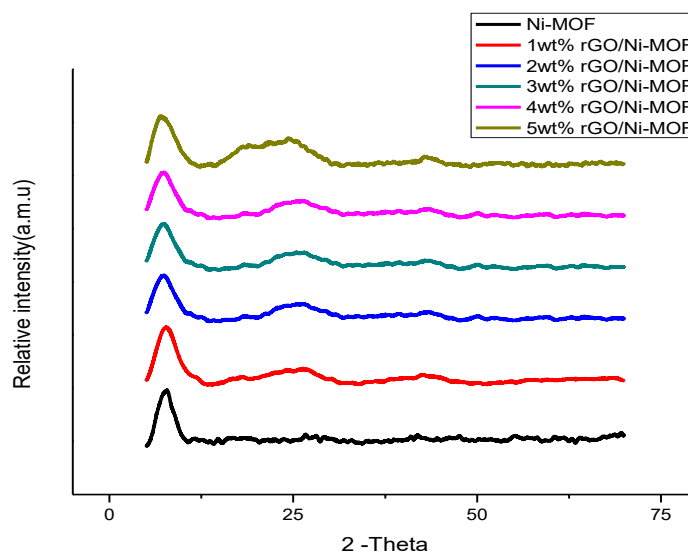
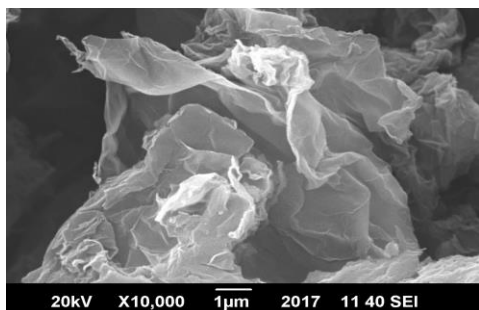


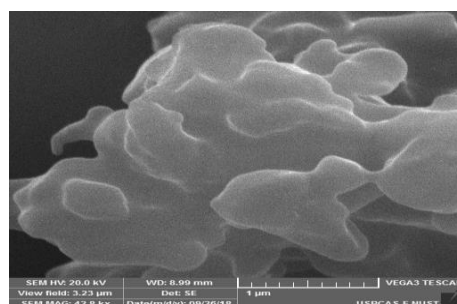
**Figure 4.1. X-ray diffraction of Ni MOF and its composites with rGO (1wt%, 2wt%, 3wt%, 4wt% and 5 wt %)**

#### 4.1.2. Scanning electron microscopy

Shapes and morphologies of Ni MOF and its composites i.e.(1wt%rGO/Ni MOF, 2wt%rGO/Ni MOF, 3wt%rGO/Ni MOF, 4wt%rGO/Ni MOF, 5wt%rGO/Ni MOF) was investigated through scanning electron microscopy. Figure (4.2) shows the successful synthesis of Ni MOF (a), rGO (b) and its composites (c-g), the images precisely shows that nano sheets of Ni MOF are embedded in to the wrinkled sheets of reduced graphene oxides [88, 92].

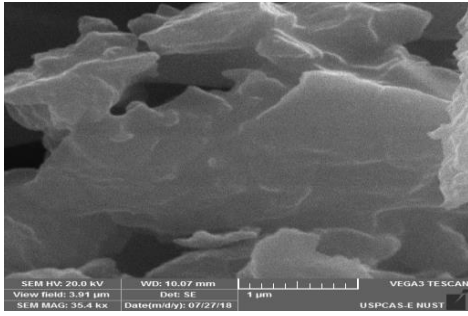


**a**

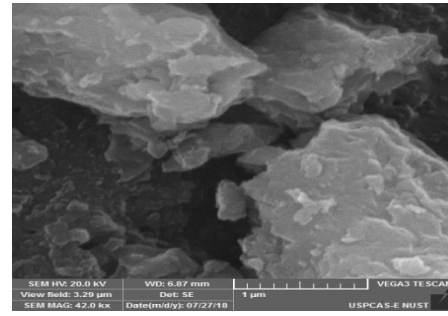


**b**

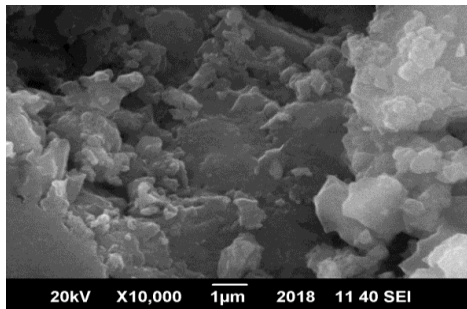




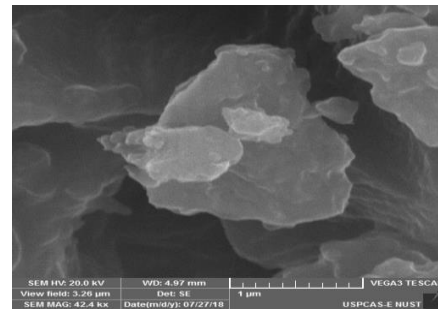
c



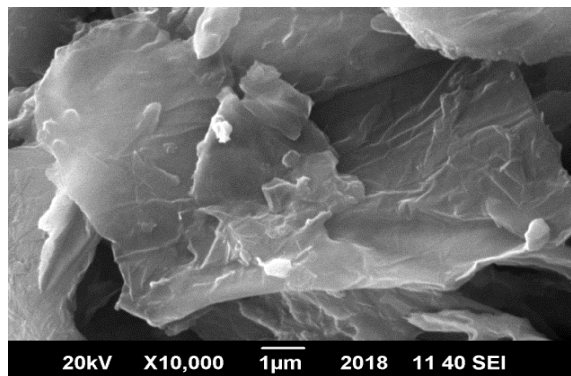
d



e



f

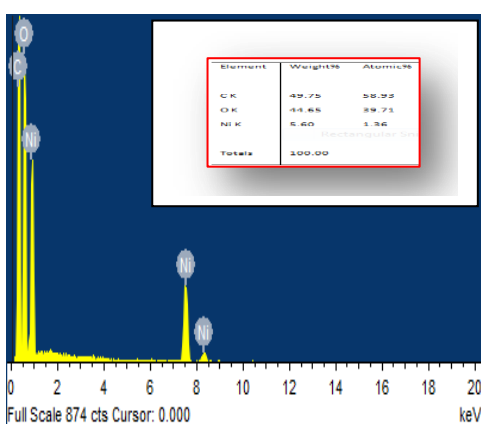


g

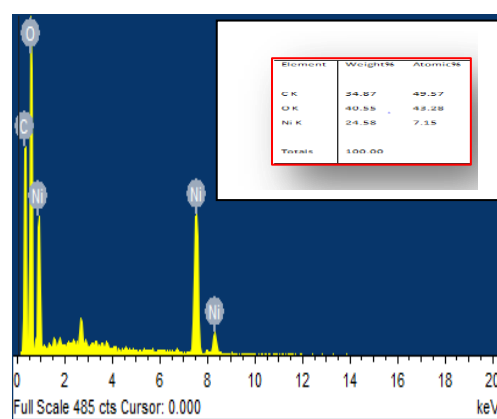
**Figure 4.2.** SEM images of Ni MOF (a) rGO (b) 1wt% rGO/Ni MOF, (c) 2wt% rGO/Ni MOF (d) 3wt% rGO/Ni MOF (e) 4wt% rGO/Ni MOF (f) 5wt% rGO/Ni MOF (g)

#### 4.1.4. Energy dispersive spectroscopy

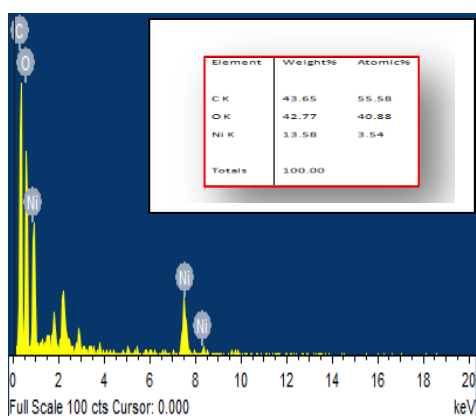
The presence of elements in as synthesized Ni MOF and its composites with rGO i.e. (1w% rGO/ Ni MOF, 2w% rGO/ Ni MOF, 3w% rGO/ Ni MOF, 4w% rGO/ Ni MOF and 5w% rGO/ Ni MOF) were studied by (EDS). Figure (4.3) illustrate the presence of Ni, C, and O without any impurity. This analysis may also confirm the synthesis of Ni MOF and their composites.



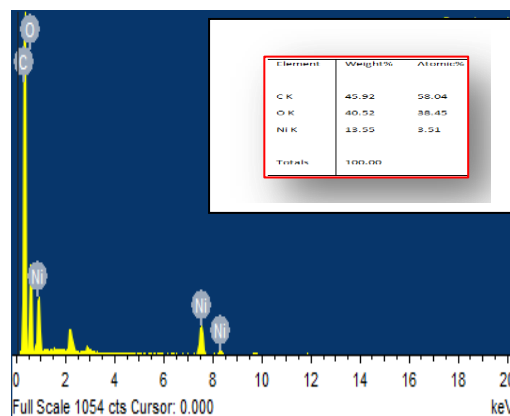
a



b



c



d

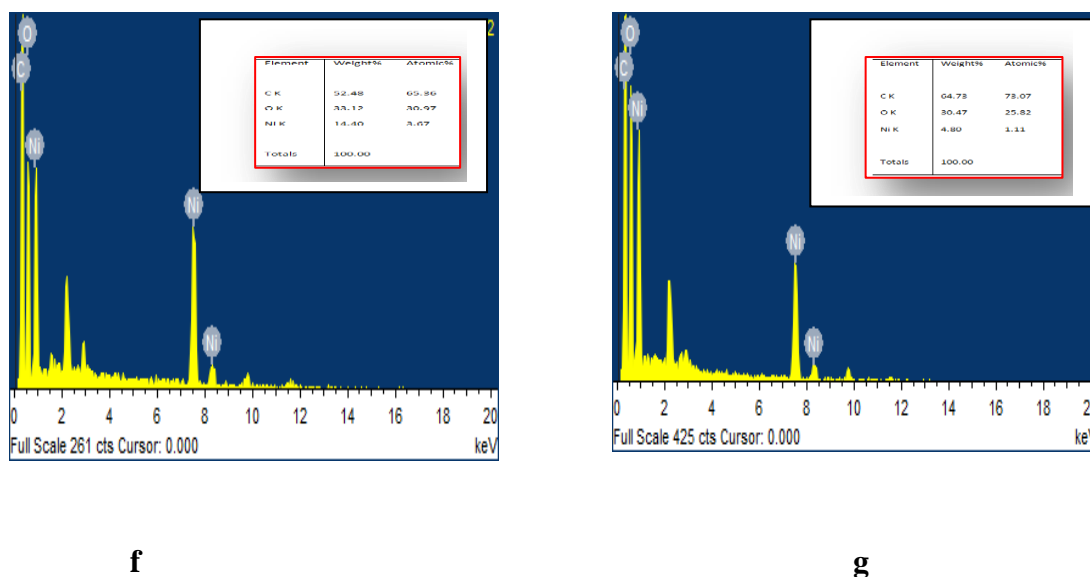


**Figure 4.3.EDX results of Ni MOF (a) 1wt%rGO/Ni MOF, (b) 2wt% rGO/Ni MOF (c) 3wt%rGO/Ni MOF (d) 4wt% rGO/Ni MOF (e) 5wt%rGO /Ni MOF (f) Ni MOF)**

#### **4.1.5. Fourier transform infrared analysis**

The presence of various functional groups in Ni MOF and its composites with rGO were investigated by FTIR analysis figure (4.4). The Sharp band at  $1392\text{-}1380\text{cm}^{-1}$  and  $1622\text{-}1579\text{cm}^{-1}$  illustrate C=O symmetric and asymmetric stretching, Further COOH group in BDC (linker) deprotonation was confirmed by absence of absorption peak in  $1715\text{-}1680\text{cm}^{-1}$  region. Moreover BDC linker C-H out of plan and in plan bending observes at  $1008\text{-}748\text{cm}^{-1}$ . So IR absorption of prepared Ni MOF and its composites with rGO confirms their successful preparation [93].

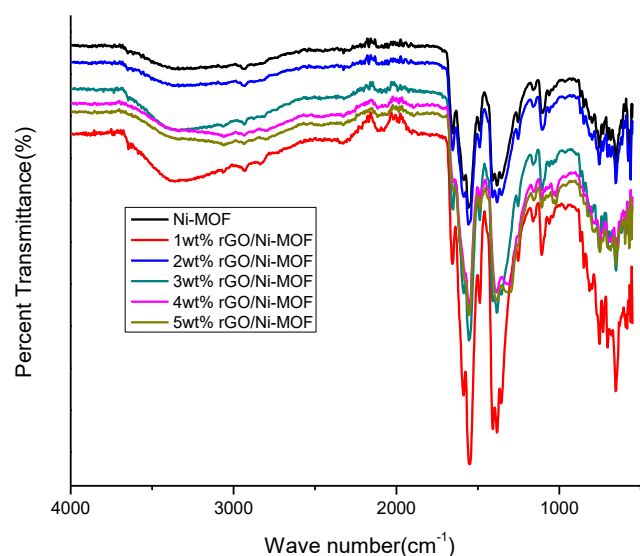


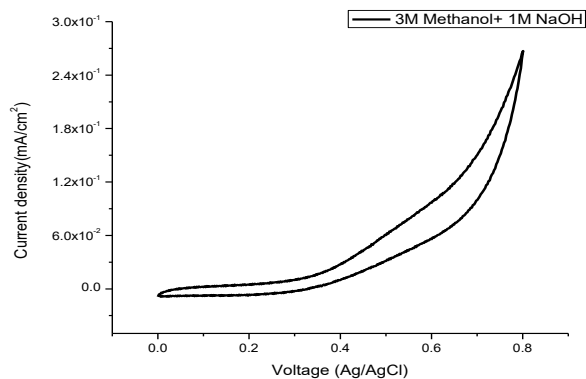
**Figure 4.4. FTIR analysis of Ni MOF and its composites with (1wt%, 2wt%, 3wt%, 4wt% and 5wt %) rGO/ Ni MOF**

## 4.2. Electrochemical characterizations

All electrochemical experiments were done in 3M methanol and 1M NaOH by using three electrode systems in which glassy carbon electrode act as working electrode, silver-silver chloride as reference electrode and Pt wire a counter electrode. Moreover methanol solution and NaOH act as fuel and supporting electrolytes. The scan was taken for both modified and bare GCE.

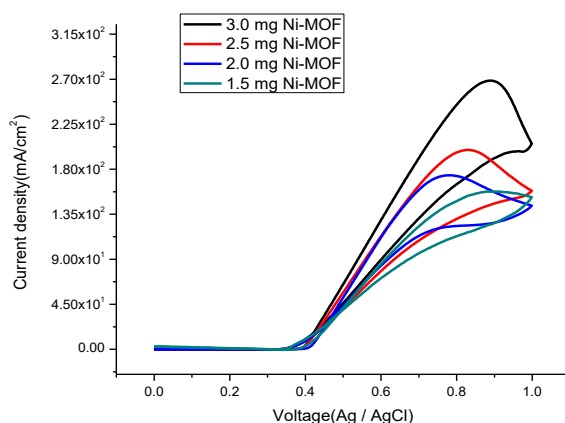
### 4.2.1. Cyclic voltammetry

The electrochemical analysis initiated with Bare GCE scan in 3 electrode system filled with 3M methanol and 1M NaOH. NaOH act as supporting electrode and their role is quite significant in controlling the population of charged ions. As a result the system counts a chunk of charged species per second and giving off a reliable current density value at a point of scan. The bare GCE current density is just 0.013 mA/cm<sup>2</sup> at 0.6V as shown in figure (4.5)



**Figure 4.5. Cyclic voltammogram of bare GCE**

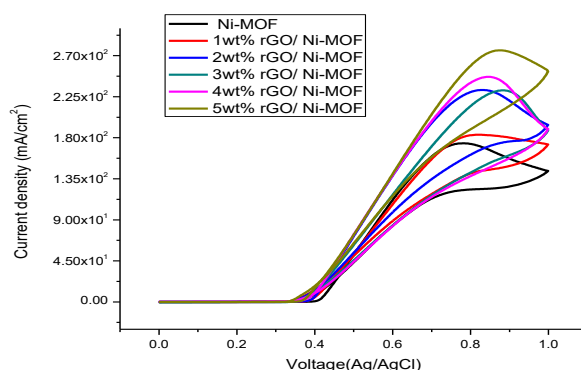
Now working electrode GCE was modified with different concentration of Ni MOF (1.5mg -3.0mg), the comparative results of this catalyst Ni-MOF at various concentrations are shown in Figure (4.6). Shows an increase in current density with increasing catalysts concentration at voltage range from (0.6-1.0V). Increasing concentration of the catalysts increases the current density this is because the surface area for electrochemical reaction increases with increasing concentration of the same catalysts and the conductivity increases accordingly. Moreover activation energy of these catalysts for MOR decreases as well. Among all the same catalysts different concentrations (3.0mg) showed a higher current density at about 0.9V Figure (4.6) this is associated with clustering of catalysts at higher catalysts concentration and thus charge transfer takes place at higher voltage.



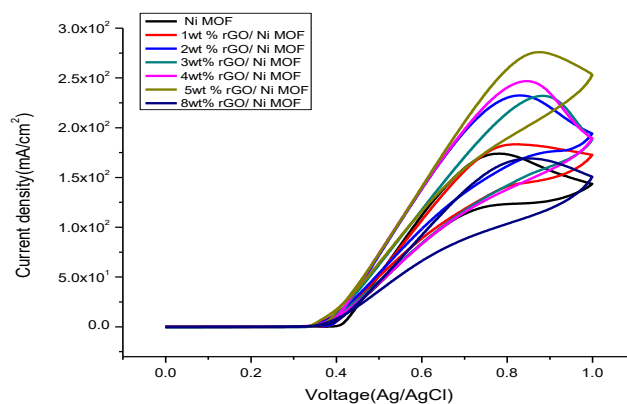
**Figure 4.6. Cyclic voltammogram with different concentrations of NiMOF**

GCE was also modified by applying one by one a thin layer of NiMOF and their composites with (1wt%, 2wt%, 3wt%, 4wt% ,5 wt %and 8wt%) reduced graphene oxides and the results were compared with Ni MOF itself figure (4.7)all the catalyts concentration was 2mg at scan rate 50mV/s. In cyclic voltammogram comparative results were taken by running a potentiostatic scan of modified GCE and bare GCE electrode in 3M methanol and 1M NaOH to observe the change in response of catalyts upon adding rGO. The sample with higher rGO concentration has enhanced electro catalytic activity toward MOR [94]. Among all the as prepared composites 5wt% rGO/NiMOF show highest current density ( $275\text{mA}/\text{cm}^2$ ) than other prepared composites i.e.( $210\text{mA}/\text{cm}^2$ ,  $230\text{mA}/\text{cm}^2$ , $183.28\text{mA}/\text{cm}^2$ , $172\text{mA}/\text{cm}^2$ ) at 50mV/s. These results suggested that Ni MOF particles deposition on rGO are more feasible to oxidation reaction and needs smaller activation energy this is all due to rGO highest conductivity [95].

As for 8wt% are concerned the efficiency as expected was not satisfactory behind this one possible reason may be rGO clustering leading toward blockage of space the other reason may be accumulation of charges on larger surface of rGO[96].At point May results in lower current density at 50mV/s, thus increasing rGO concentration after a certain limit has a negative effect on current density. In contrast to 5wt% rGO/NiMOF current density ( $275.85\text{mA}$ ), 8wt% rGO exhibits  $169\text{mA}/\text{cm}^2$  at 50mV/s as shown in figure (4.8)

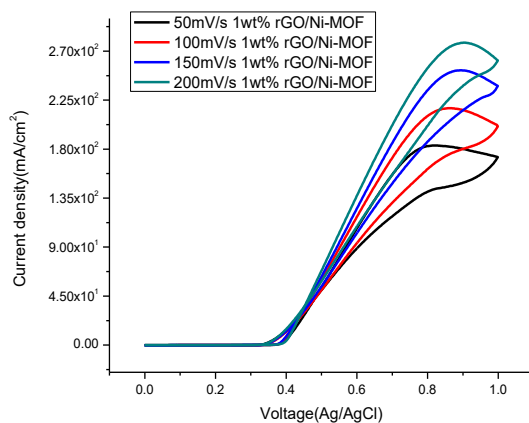


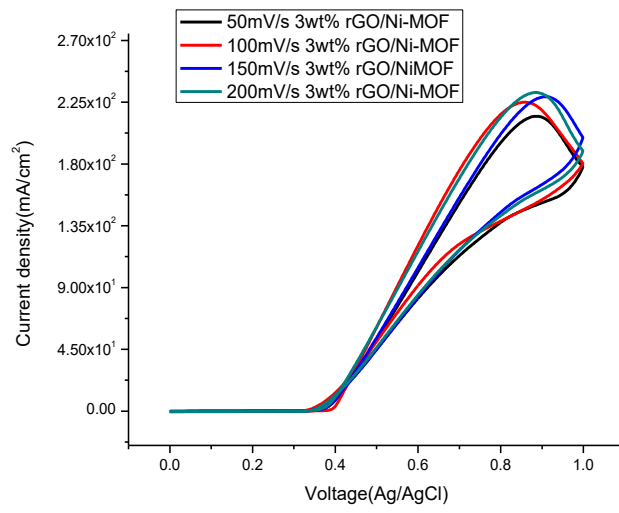
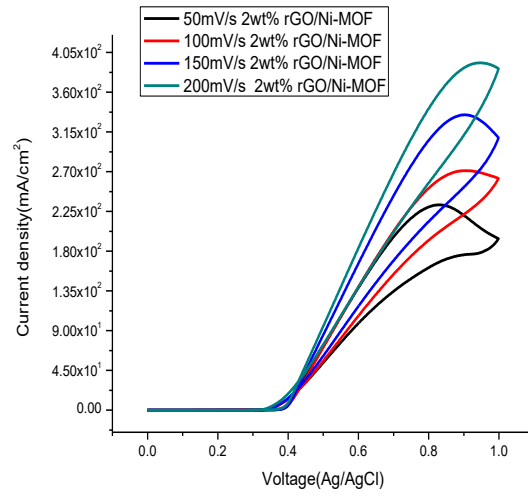
**Figure 4.7. Cyclic voltammogram of Ni MOF composites (1wt% rGO/Ni MOF, 2wt% rGO/Ni MOF, 3wt% rGO/Ni MOF, 4wt%rGO/Ni MOF and 5wt%rGO/ Ni MOF)**



**Figure 4.8. Cyclic voltammogram of Ni MOF and their composites (1wt%, 2wt%, 3wt%, 4wt%, 5wt%,8wt %)rGO/Ni MOF in 1 M NaOH and 3M methanol at 50mV/s.**

The scan rate effect was also studied for Ni-MOF and its composites with (1wt%, 2wt%, 3wt%, 4wt% and 5wt %) with rGO at various scan rates (50mV/s, 100mV/s, 150mV/s and 200mV/s). At faster scan rate the current density increases because of the reason that higher scan rate does not allow the non electro active reaction components to be reduced or oxidized in to product [97], Thus only electro active reaction components giving off the higher current density values. We examine a gradual increase in current density values, as shown in figure (4.9)







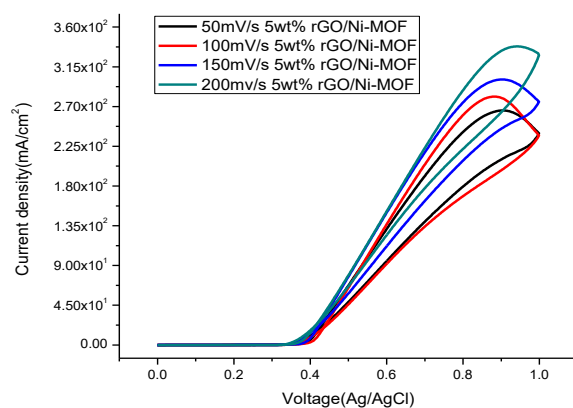
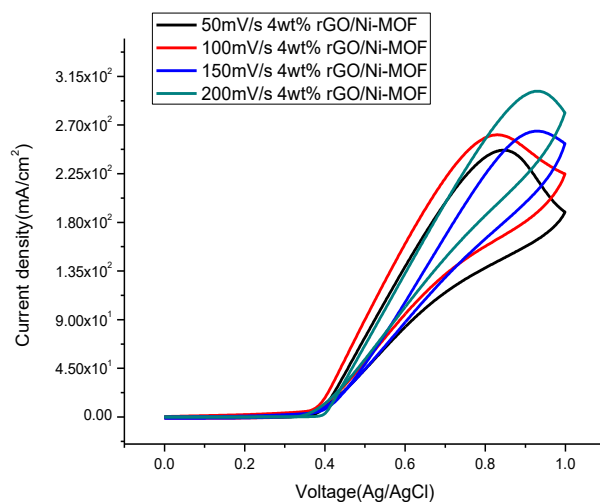
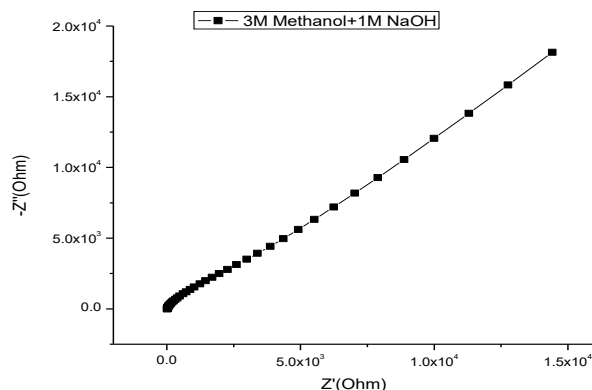


**Figure 4.9. Cyclic voltammogram of Ni MOF and its composites with 1wt%, 2wt%, 3wt%, 4wt% and 5wt% rGO at different scan rates (50mV/s-200mV/s) in 1 M NaOH and 3 M methanol**

#### 4.2.2. Electrochemical impedance spectroscopy

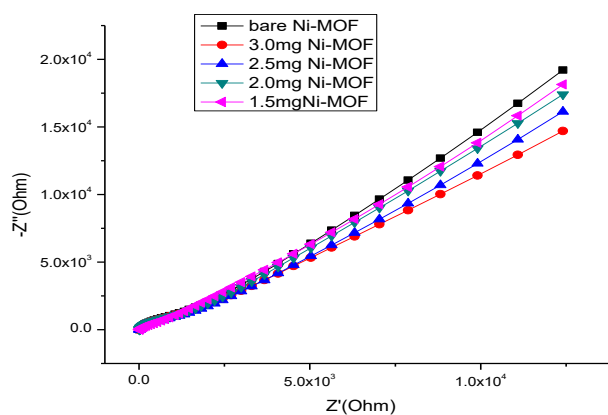
Electrochemical impedance spectroscopy is one of the excellent techniques used to analyze the electric conductance of catalytic material [98]. Electrochemical impedance in EIS was measured using same three electrode systems in 3M methanol and 1M NaOH by applying potentiostatic mode with modified and bare GCE. During the calculation of circuit electrochemical impedance in electrochemical studies the resistance between working electrode and reference electrode must be analyzed.

However, solution resistance is a dominating factor. Plot of modified GCE among real and imaginary impedance exhibits curve in lower frequency area although it is linear with bare GCE shown in figure (4.10)



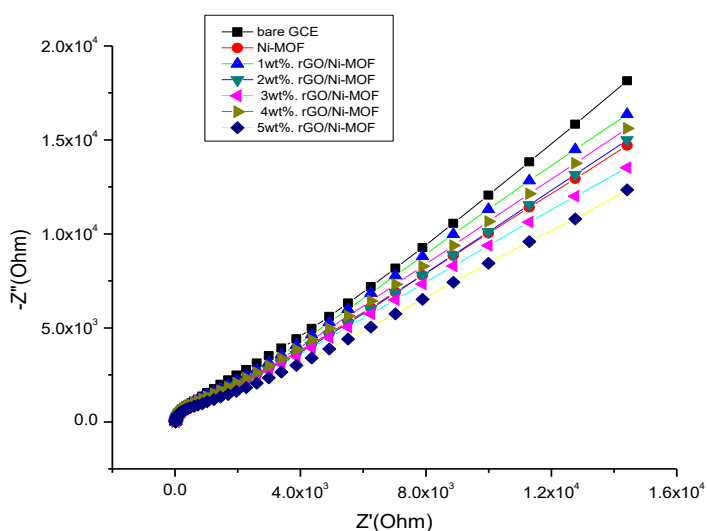
**Figure 4.10. Nyquist Plot of bare glassy carbon electrode in 1M NaOH and 3 M methanol**

Impedance value is effected by different at different concentration of Ni-MOF figure (4.11) at higher concentration of MOF the charges pass smoothly without experience much resistance, this recommended that at higher concentration of catalyst can decrease the distance between electrode surface area and catalyst layer thus toward diffusion charges transfer faces lower resistance.



**Figure 4.11. Nyquist Plots of Ni MOF at various concentrations in 1M NaOH and 3M methanol**

The impedance studies with composites of Ni-MOF were done as well in which reduced graphene oxide concentration effects on overall impedance of the system under investigation figure (4.12). The increasing concentration of rGO in composites gets lowers the impedance of charges. Moreover the equivalent results shows a tremendous decrease in the overall impedance and clearly shows that reduced graphene oxide has major contribution toward charge transfer in diffusion controlled mechanism and in addition reduced graphene oxide also contribute in the overall catalyst conductivity.



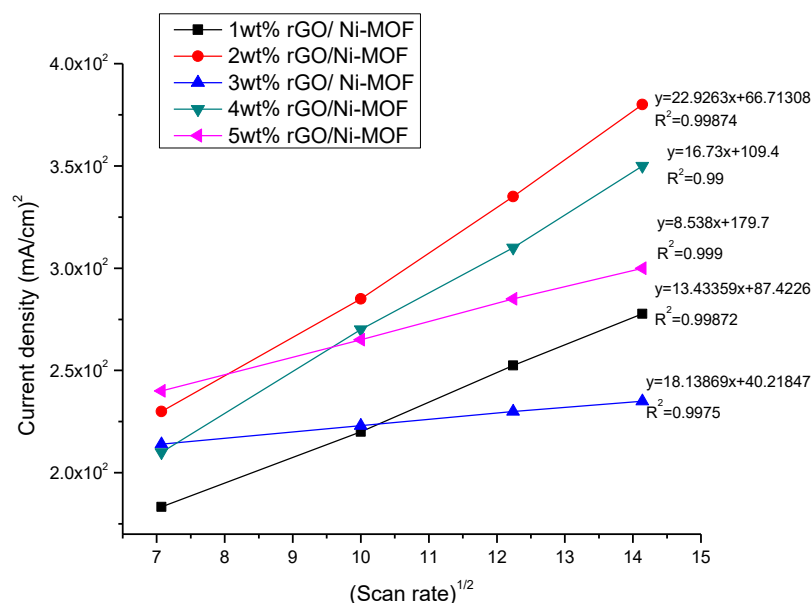
**Figure 4.12.** Nyquist plots of Bare GCE, Ni MOF and its composites 1wt%rGO/ Ni MOF, 2wt% rGO/Ni MOF, 3wt% rGO/Ni MOF, 4wt% rGO/Ni MOF and 5wt% rGO/ Ni MOF in 1M NaOH and 3M methanol.

Figure (4.13) shows a linear relationship between peak current densities of the prepared catalysts and square root of scan rate. This plot indicates the diffusion controlled process of the system which is predominant over increased value of scan rates. Moreover, by measuring the linearity and rate constant of the charge transfer between electrode and surface deposited layer the diffusion coefficient (D) and transfer coefficient ( $\alpha$ ) can be determined.

Diffusion coefficient (D) can be calculated via *Randles Sevcik* equation [99]

$$i_p = (2.99 \times 10^5) n(\alpha n_a)^{1/2} ACD^{1/2} v^{1/2}$$

For all the as prepared catalysts the diffusion coefficient value calculated as  $(2.72 \times 10^{-9} \text{ cm}^2\text{s}^{-1})$  for 5wt%,  $(2.17 \times 10^{-9} \text{ cm}^2\text{s}^{-1})$  for 4wt%,  $(1.92 \times 10^{-9} \text{ cm}^2\text{s}^{-1})$  for 3wt%,  $(1.93 \times 10^{-9} \text{ cm}^2\text{s}^{-1})$  for 2wt%,  $(1.20 \times 10^{-9} \text{ cm}^2\text{s}^{-1})$  for 1wt% and  $(1.08 \times 10^{-9} \text{ cm}^2\text{s}^{-1})$  Ni-MOF. These values indicate diffusion controlled mechanism followed by the system.



**Figure 4.13.** Plots of square of scan root vs. peak current density for Ni MOF and its composites ( 1wt%, 2wt%, 3wt%, 4wt%, 5wt% ) rGO/Ni MOF

### 4.3. Chronoamperometry

The stability of the as prepared electro catalysts were investigated within the same cell containing three electrodes i.e. glassy carbon electrode (working electrode), Pt wire (counter electrode) and Ag /AgCl (reference electrode) and 1MNaOH+3M methanol by chronoamperometry at voltage 0.9V. Figure (4.14) illustrate the chronoamperometry curves of prepared electro catalysts. These curves indicates that in comparison to Ni MOF its composites with rGO show stability over as period of time 3600s, But all the prepared catalysts were not 100% stable they show a rapid decline in current in initial 60s this is because of reaction intermediate formation mainly carbon monoxide [100, 101], after the first 60s the % stability were recorded for Ni MOF and its composites with rGO are (60%) for 5wt%, followed by 2wt%

(55%), 1wt% (50%), 4wt% (38%), 3wt% (29%) and Ni MOF (29%), over the course of time (3600s) all composites show stability except Ni MOF show a rapid decline.

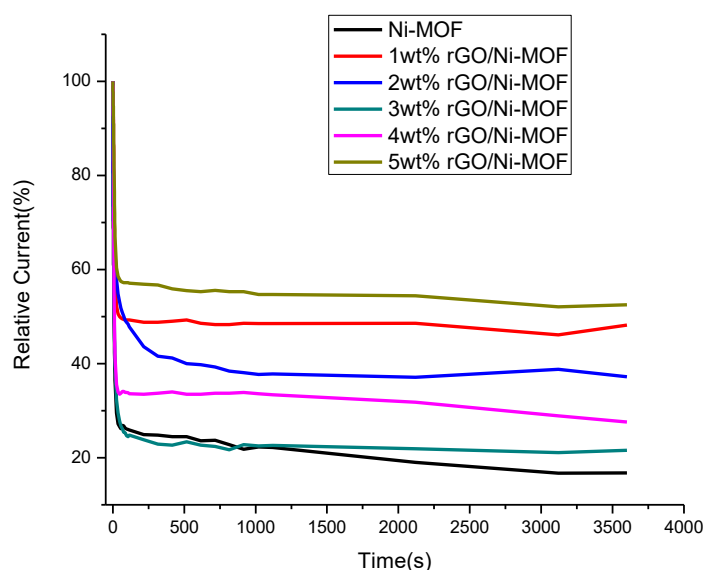


**Figure 4.14. Chronoamperometry curves for Ni MOF and its composites (1wt%, 2wt%, 3wt%, 4wt%, 5wt %) rGO /Ni MOF in 3M methanol and 1 M NaOH**

#### 4.4. Tafel studies

Figure (4.15) represents Tafel plots of as prepared catalysts, by comparing over potential with current density these plots illustrate the electrochemical kinetics. Pt (commercially available material) shows these curves at lowest voltage (0.0V) in contrast to this material, all the as prepared composites of Ni MOF with rGO (1wt%, 2wt%, 3wt%, 4wt% and 5wt %), 5wt% rGO/Ni MOF shows lowest over potential, it suggested that rGO incorporation in to Ni MOF may increase the surface area and facilitates the reactants accessibility to electrode as a result it capture more ions and exhibits greater reaction activity for methanol oxidation [5, 102, 103].

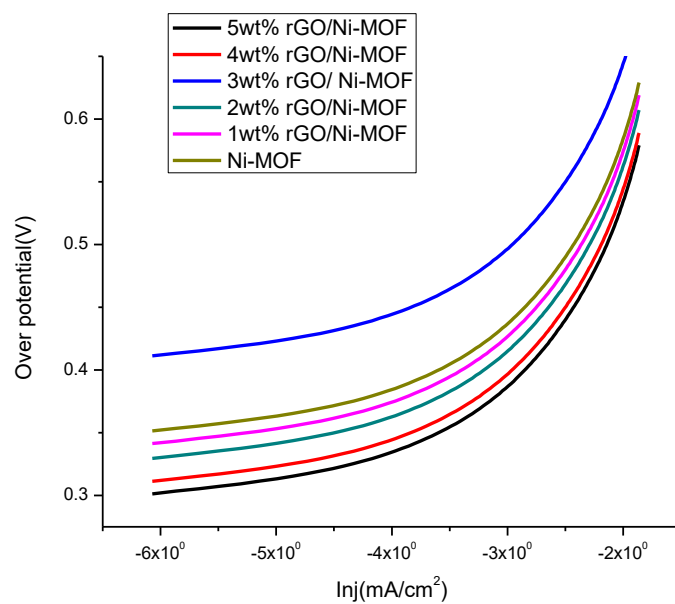


**Figure 4.15. Tafel plots for Ni MOF and their composites with rGO in 3M methanol and 1 M NaOH**

The electrochemical properties of the following catalytic materials in comparison with reported electro catalyst can be summarized in the following given tabular form.

Catalytic materials	Methanol Conc. (M)	Scan rate (mV/sec)	Anodic potential (V)	Peak current density (mA/cm <sup>2</sup> )	References
Co-MOF/GO	3	50	0.10	29.1	[5]
NiCo <sub>2</sub> O <sub>4</sub> - NC	0.5	10	0.6	134	[104]
NiCo <sub>2</sub> O <sub>4</sub> - NS	0.5	10	0.6	111	[104]
Pt-Ni	1	-	0.8	265	[105]
NiCo <sub>2</sub> O <sub>4</sub> MWCNTs	2	50	0.664	247.9	[106]
Pt-Pd/C	1	50	0.6	280	[107]
Ni MOF	3	50	0.78	174	This work
1wt% rGO/Ni MOF	3	50	0.8	183.28	This work
2wt% rGO/Ni MOF	3	50	0.8	232.4	This work
3wt% rGO/Ni MOF	3	50	0.8	232.0	This work
4wt% rGO/Ni MOF	3	50	0.8	246.71	This work
5wt%rGO/Ni MOF	3	50	0.8	275.85	This work

**Table 4.1. Comparison of scan rates, current densities and voltages with Ni MOF and its composites (1wt%, 2wt%, 3wt%, 4wt%, 5wt %) rGO/Ni MOF with reported catalysts**

# CHAPTER 5

## Conclusion and Future recommendations

### 5.1. Conclusion

Ni MOF and their composites with rGO i.e. (1wt%, 2wt%, 3wt%, 4wt% and 5wt %) have been prepared through hydrothermal method by incorporation of reduce graphene oxide (rGO) into Ni MOF sheets. Lab prepared catalysts morphology and presence of specific elements were confirmed by SEM and EDS analysis respectively. Functional groups were identified by FTIR spectroscopic studies. Furthermore, the incorporation of Ni MOF with rGO was confirmed by performing XRD of composites.

The electrochemical properties of lab prepared catalysts for oxidation reaction of methanol were tested by cyclic voltammetry, electron impedance spectroscopy and chronoamperometry by using three electrode systems in 3M methanol and 1M NaOH. Among all prepared series of composites 5wt% rGO/ Ni MOF at scan rate 50mv/s shows highest current density ( $275.85\text{mA/cm}^2$ ) with low impedance value. These results are suggestive of the fact that rGO enhances surface area and conductivity of Ni MOF. These remarkable properties of Ni MOF catalysts series make them a promising alternative to platinum in electrocatalysis field.

### 5.2. Future recommendations

The study of environmental friendly Ni MOF and their rGO based composites lead toward a promising future of these materials in DMFCs for oxidation of methanol. Thus this work can be further expended by introducing nanomaterials like nano particles and nanotubes into metal organic framework. Furthermore studying the concentration effect of Ni MOF on current density the voltage shift occur, also the addition of rGO more than that 5wt% i.e. 8wt% shows least activity towards MOR. This may be associated with the clustering of rGO at higher concentration or accumulation of charges on rGO surface. We can investigate the following features by



performing the analysis with low variation in rGO amount for composites and control the voltage shift at higher concentration of catalytic material. Moreover, we can use the prepared material for CO<sub>2</sub> capturing.

# References

- [1] S. Pathak, "Energy Crisis; A Review," *International Journal of Engineering Research and Applications*, vol. 4, pp. 845-851, 2014.
- [2] S. Shafiee and E. Topal, "When will fossil fuel reserves be diminished?," *Energy policy*, vol. 37, pp. 181-189, 2009.
- [3] M. N. Qureshi, "ENERGY CRISIS IN PAKISTAN: A THREAT TO NATIONAL SECURITY."
- [4] A. Aqeel and M. S. Butt, "The relationship between energy consumption and economic growth in Pakistan," *Asia-Pacific Development Journal*, vol. 8, pp. 101-110, 2001.
- [5] R. Mehek, N. Iqbal, T. Noor, H. Nasir, Y. Mehmood, and S. Ahmed, "Novel Co-MOF/Graphene Oxide Electrocatalyst for Methanol Oxidation," *Electrochimica Acta*, vol. 255, pp. 195-204, 2017.
- [6] B. S. Baker and H. G. Ghezal-Ayagh, "Fuel cell system," ed: Google Patents, 1985.
- [7] P. J. Damiano, "Fuel cell structure," ed: Google Patents, 1978.
- [8] L. Carrette, K. A. Friedrich, and U. Stimming, "Fuel cells: principles, types, fuels, and applications," *ChemPhysChem*, vol. 1, pp. 162-193, 2000.
- [9] L. J. Blomen and M. N. Mugerwa, *Fuel cell systems*: Springer Science & Business Media, 2013.
- [10] H. Vaghari, H. Jafarizadeh-Malmiri, A. Berenjian, and N. Anarjan, "Recent advances in application of chitosan in fuel cells," *Sustainable Chemical Processes*, vol. 1, p. 16, 2013.
- [11] J. Y. Lee, H. H. Lee, J. H. Lee, and D. M. Kim, "Alkaline fuel cell," ed: Google Patents, 1997.
- [12] N. Mitsuda, J. i. Hosokawa, and H. Shioda, "Phosphoric acid fuel cell," 1987.
- [13] Y. Wang, K. S. Chen, J. Mishler, S. C. Cho, and X. C. Adroher, "A review of polymer electrolyte membrane fuel cells: technology, applications, and needs on fundamental research," *Applied energy*, vol. 88, pp. 981-1007, 2011.
- [14] S. Gottesfeld and T. A. Zawodzinski, "Polymer electrolyte fuel cells," *Advances in electrochemical science and engineering*, vol. 5, pp. 195-301, 1997.

- [15] A. Aman, R. Gentile, Y. Xu, and N. Orlovskaya, "Parametric Study of Electrolyte-Supported Planar Button Solid Oxide Fuel Cell."
- [16] R. M. Ormerod, "Solid oxide fuel cells," *Chemical Society Reviews*, vol. 32, pp. 17-28, 2003.
- [17] A. L. Dicks, "Molten carbonate fuel cells," *Current Opinion in Solid State and Materials Science*, vol. 8, pp. 379-383, 2004.
- [18] Y. Suzuki, H. Usui, Y. Kitade, and N. Yoshikawa, "Microbial fuel cell system," ed: Google Patents, 2018.
- [19] A. Parkash, "Microbial fuel cells: a source of bioenergy," *J Microb Biochem Technol*, vol. 8, pp. 247-255, 2016.
- [20] K. Matsuoka, Y. Sato, and K. Kawano, "Direct methanol fuel cell system," ed: Google Patents, 2004.
- [21] N. V. Long, C. M. Thi, M. Nogami, and M. Ohtaki, "Novel Pt and Pd Based Core-Shell Catalysts with Critical New Issues of Heat Treatment, Stability and Durability for Proton Exchange Membrane Fuel Cells and Direct Methanol Fuel Cells," in *Heat Treatment-Conventional and Novel Applications*, ed: InTech, 2012.
- [22] Y. Muramatsu, H. Kohda, and S. Shiozawa, "Direct methanol fuel cell system," ed: Google Patents, 2006.
- [23] T. R. Cook, Y.-R. Zheng, and P. J. Stang, "Metal–organic frameworks and self-assembled supramolecular coordination complexes: comparing and contrasting the design, synthesis, and functionality of metal–organic materials," *Chemical reviews*, vol. 113, pp. 734-777, 2012.
- [24] C. Carbonell Fernández, "Surface structuration of metal-organic frameworks using tip-based lithographies," 2015.
- [25] G. Maurin, C. Serre, A. Cooper, and G. Férey, "The new age of MOFs and of their porous-related solids," *Chemical Society Reviews*, vol. 46, pp. 3104-3107, 2017.
- [26] K. Meyer, P. Lorenz, B. Böhl-Kuhn, and P. Klobes, "Porous solids and their characterization methods of investigation and application," *Crystal research and technology*, vol. 29, pp. 903-930, 1994.
- [27] O. Shekhah, J. Liu, R. Fischer, and C. Wöll, "MOF thin films: existing and future applications," *Chemical Society Reviews*, vol. 40, pp. 1081-1106, 2011.

- [28] O. Fleker, A. Borenstein, R. Lavi, L. Benisvy, S. Ruthstein, and D. Aurbach, "Preparation and properties of metal organic framework/activated carbon composite materials," *Langmuir*, vol. 32, pp. 4935-4944, 2016.
- [29] I. N. Najm, V. L. Snoeyink, B. W. Lykins Jr, and J. Q. Adams, "Using powdered activated carbon: a critical review," *Journal-American Water Works Association*, vol. 83, pp. 65-76, 1991.
- [30] S. Montalvo, L. Guerrero, R. Borja, E. Sánchez, Z. Milán, I. Cortés, *et al.*, "Application of natural zeolites in anaerobic digestion processes: a review," *Applied Clay Science*, vol. 58, pp. 125-133, 2012.
- [31] B. Liu, H. Shioyama, T. Akita, and Q. Xu, "Metal-organic framework as a template for porous carbon synthesis," *Journal of the American Chemical Society*, vol. 130, pp. 5390-5391, 2008.
- [32] S. L. James, "Metal-organic frameworks," *Chemical Society Reviews*, vol. 32, pp. 276-288, 2003.
- [33] C. Dey, T. Kundu, B. P. Biswal, A. Mallick, and R. Banerjee, "Crystalline metal-organic frameworks (MOFs): synthesis, structure and function," *Acta Crystallographica Section B: Structural Science, Crystal Engineering and Materials*, vol. 70, pp. 3-10, 2014.
- [34] A. Dhakshinamoorthy and H. Garcia, "Catalysis by metal nanoparticles embedded on metal-organic frameworks," *Chemical Society Reviews*, vol. 41, pp. 5262-5284, 2012.
- [35] N. Stock and S. Biswas, "Synthesis of metal-organic frameworks (MOFs): routes to various MOF topologies, morphologies, and composites," *Chemical reviews*, vol. 112, pp. 933-969, 2011.
- [36] D. Andirova, C. F. Cogswell, Y. Lei, and S. Choi, "Effect of the structural constituents of metal organic frameworks on carbon dioxide capture," *Microporous and Mesoporous Materials*, vol. 219, pp. 276-305, 2016.
- [37] T. K. Chandan Dey, Bishnu P. Biswal, Arijit Mallick\*and Rahul Banerjee\*, "Crystalline metal-organic frameworks (MOFs):synthesis, structure and function," Received 16 July 2013.
- [38] P. V. V. R. Seetharaj 1, P. Arya 1, S. Mathew 1,2,\* , "Dependence of solvents, pH, molar ratio and," Received 12 August 2015; accepted 8 January 2016.

- [39] N. Stock and S. Biswas, "Synthesis of metal-organic frameworks (MOFs): routes to various MOF topologies, morphologies, and composites," *Chem Rev*, vol. 112, pp. 933-69, Feb 8 2012.
- [40] Y.-R. Lee, J. Kim, and W.-S. Ahn, "Synthesis of metal-organic frameworks: A mini review," *Korean Journal of Chemical Engineering*, vol. 30, pp. 1667-1680, 2013.
- [41] J. K. Yu-Ri Lee, and Wha-Seung Ahn†, "Synthesis of metal-organic frameworks: A mini review," Received 10 May 2013 • accepted 30 July 2013).
- [42] W.-J. Son, J. Kim, J. Kim, and W.-S. Ahn, "Sonochemical synthesis of MOF-5," *Chemical Communications*, pp. 6336-6338, 2008.
- [43] C. Dey, T. Kundu, B. P. Biswal, A. Mallick, and R. Banerjee, "Crystalline metal-organic frameworks (MOFs): synthesis, structure and function," *Acta Crystallogr B Struct Sci Cryst Eng Mater*, vol. 70, pp. 3-10, Feb 2014.
- [44] H.-L. Jiang and Q. Xu, "Porous metal-organic frameworks as platforms for functional applications," *Chemical Communications*, vol. 47, pp. 3351-3370, 2011.
- [45] P. Kumar, A. Deep, and K.-H. Kim, "Metal organic frameworks for sensing applications," *TrAC Trends in Analytical Chemistry*, vol. 73, pp. 39-53, 2015.
- [46] J. H. Seinfeld and S. N. Pandis, *Atmospheric chemistry and physics: from air pollution to climate change*: John Wiley & Sons, 2012.
- [47] S. Ma and H.-C. Zhou, "Gas storage in porous metal-organic frameworks for clean energy applications," *Chemical Communications*, vol. 46, pp. 44-53, 2010.
- [48] D. Britt, D. Tranchemontagne, and O. M. Yaghi, "Metal-organic frameworks with high capacity and selectivity for harmful gases," *Proceedings of the National Academy of Sciences*, vol. 105, pp. 11623-11627, 2008.
- [49] S. Saufi and A. Ismail, "Fabrication of carbon membranes for gas separation—a review," *Carbon*, vol. 42, pp. 241-259, 2004.
- [50] T. M. Stark, "Gas separation by adsorption process," ed: Google Patents, 1966.
- [51] T. H. Bae, J. S. Lee, W. Qiu, W. J. Koros, C. W. Jones, and S. Nair, "A high-performance gas-separation membrane containing submicrometer-sized

- metal–organic framework crystals," *Angewandte Chemie*, vol. 122, pp. 10059-10062, 2010.
- [52] S. Japip, H. Wang, Y. Xiao, and T. S. Chung, "Highly permeable zeolitic imidazolate framework (ZIF)-71 nano-particles enhanced polyimide membranes for gas separation," *Journal of Membrane Science*, vol. 467, pp. 162-174, 2014.
- [53] S. T. Meek, J. A. Greathouse, and M. D. Allendorf, "Metal-organic frameworks: A rapidly growing class of versatile nanoporous materials," *Advanced Materials*, vol. 23, pp. 249-267, 2011.
- [54] D. Farrusseng, *Metal-organic frameworks: applications from catalysis to gas storage*: John Wiley & Sons, 2011.
- [55] D. Zhao, S. Tan, D. Yuan, W. Lu, Y. H. Rezenom, H. Jiang, *et al.*, "Surface functionalization of porous coordination nanocages via click chemistry and their application in drug delivery," *Advanced Materials*, vol. 23, pp. 90-93, 2011.
- [56] R. C. Huxford, J. Della Rocca, and W. Lin, "Metal–organic frameworks as potential drug carriers," *Current opinion in chemical biology*, vol. 14, pp. 262-268, 2010.
- [57] P. Horcajada, T. Chalati, C. Serre, B. Gillet, C. Sebrie, T. Baati, *et al.*, "Porous metal-organic-framework nanoscale carriers as a potential platform for drug delivery and imaging," *Nat Mater*, vol. 9, pp. 172-8, Feb 2010.
- [58] E. g. U. H. Y. A.-E. Andrei A. Bunaciu, "X-Ray Diffraction: Instrumentation and Applications," 01 Apr 2015.
- [59] B. E. Warren, *X-ray Diffraction*: Courier Corporation, 1990.
- [60] U. Holzwarth and N. Gibson, "The Scherrer equation versus the 'Debye-Scherrer equation'," *Nature nanotechnology*, vol. 6, p. 534, 2011.
- [61] B. C. Smith, *Fundamentals of Fourier Transform Infrared Spectroscopy*: CRC Press,, 2011.
- [62] L. Reimer, *Scanning electron microscopy: physics of image formation and microanalysis* vol. 45: Springer, 2013.
- [63] P. T. Kissinger and W. R. Heineman, "Cyclic voltammetry," *Journal of Chemical Education*, vol. 60, p. 702, 1983.
- [64] M. A. a. B. K. A. Sezai Sarac\*, "Electrochemical Impedance Spectroscopic Study of Polyaniline," 2008.

- [65] K. Byrappa and M. Yoshimura, *Handbook of hydrothermal technology*: William Andrew, 2012.
- [66] K. B. M. Yoshimura, *Handbook of Hydrothermal Technology 2nd Edition*: Elsevier Science, 2008.
- [67] L. O. Adriana Vulcu, Gabriela Blanita, Camelia Berghian-Grosan\*, "The electrochemical behavior of a Metal-Organic Framework modified gold electrode for methanol oxidation," Received 12 May 2016 Received in revised form 10 October 2016 Accepted 11 October 2016.
- [68] R. O. a. S. R. H. Jahan Bakhsh Raoof\*, "An Electrochemical Investigation of Methanol Oxidation on Nickel Hydroxide Nanoparticles," Received 29 April 2012, Revised 7 December 2012, accepted 21 January 2013.
- [69] Y. Wang, W. Chen, D. Pan, Q. Xu, J. Ma, J. Zheng, *et al.*, "Methanol Electrooxidation Reaction in Alkaline Medium on Glassy Carbon Electrode Modified with Ordered Mesoporous Ni/Al<sub>2</sub>O<sub>3</sub>," *INTERNATIONAL JOURNAL OF ELECTROCHEMICAL SCIENCE*, vol. 12, pp. 2194-2206, 2017.
- [70] J.-H. C. Kyung-Won Park, Boo-Kil Kwon, Seol-Ah Lee, and Yung-Eun Sung\* Heung-Yong Ha and Seong-Ahn Hong Hongsun Kim and Andrzej Wieckowski\*, "Chemical and Electronic Effects of Ni in Pt/Ni and Pt/Ru/Ni Alloy Nanoparticles in Methanol Electrooxidation," Received: August 17, 2001; In Final Form: December 17, 2001.
- [71] H.-X. Zhang, C. Wang, J.-Y. Wang, J.-J. Zhai, and W.-B. Cai, "Carbon-supported Pd–Pt nanoalloy with low Pt content and superior catalysis for formic acid electro-oxidation," *The Journal of Physical Chemistry C*, vol. 114, pp. 6446-6451, 2010.
- [72] A. O. Neto, R. R. Dias, M. M. Tusi, M. Linardi, and E. V. Spinacé, "Electro-oxidation of methanol and ethanol using PtRu/C, PtSn/C and PtSnRu/C electrocatalysts prepared by an alcohol-reduction process," *Journal of Power Sources*, vol. 166, pp. 87-91, 2007.
- [73] D. Chen, Y. Zhao, X. Peng, X. Wang, W. Hu, C. Jing, *et al.*, "Star-like PtCu nanoparticles supported on graphene with superior activity for methanol electro-oxidation," *Electrochimica Acta*, vol. 177, pp. 86-92, 2015.
- [74] J.-D. Qiu, G.-C. Wang, R.-P. Liang, X.-H. Xia, and H.-W. Yu, "Controllable deposition of platinum nanoparticles on graphene as an electrocatalyst for

- direct methanol fuel cells," *The Journal of Physical Chemistry C*, vol. 115, pp. 15639-15645, 2011.
- [75] Z. He, J. Chen, D. Liu, H. Zhou, and Y. Kuang, "Electrodeposition of Pt–Ru nanoparticles on carbon nanotubes and their electrocatalytic properties for methanol electrooxidation," *Diamond and Related Materials*, vol. 13, pp. 1764-1770, 2004.
- [76] T. Deivaraj, W. Chen, and J. Y. Lee, "Preparation of PtNi nanoparticles for the electrocatalytic oxidation of methanol," *Journal of Materials Chemistry*, vol. 13, pp. 2555-2560, 2003.
- [77] L. Yang, J. Chen, X. Zhong, K. Cui, Y. Xu, and Y. Kuang, "Au@ Pt nanoparticles prepared by one-phase protocol and their electrocatalytic properties for methanol oxidation," *Colloids and Surfaces A: Physicochemical and Engineering Aspects*, vol. 295, pp. 21-26, 2007.
- [78] D. M. Ferrer, J. A. M. Banda, R. S. Rodrigo, J. Y. V. Gómez, U. P. García, P. D. Á. Vicente, *et al.*, "Electrochemical Performance of Pt/NC and Pt/rGO for Methanol Oxidation in Acid Media," *ECS Transactions*, vol. 84, pp. 41-47, 2018.
- [79] X. Li, H. Wang, H. Yu, Z. Liu, H. Wang, and F. Peng, "Enhanced activity and durability of platinum anode catalyst by the modification of cobalt phosphide for direct methanol fuel cells," *Electrochimica Acta*, vol. 185, pp. 178-183, 2015.
- [80] X. Li, L. Luo, F. Peng, H. Wang, and H. Yu, "Enhanced activity of Pt/CNTs anode catalyst for direct methanol fuel cells using Ni<sub>2</sub>P as co-catalyst," *Applied Surface Science*, vol. 434, pp. 534-539, 2018.
- [81] Y. Li, C. Liu, Y. Liu, B. Feng, L. Li, H. Pan, *et al.*, "Sn-doped TiO<sub>2</sub> modified carbon to support Pt anode catalysts for direct methanol fuel cells," *Journal of Power Sources*, vol. 286, pp. 354-361, 2015.
- [82] S. J. Zaidi, M. Bello, A. Al-Ahmed, A. B. Yousaf, and M. Imran, "Mesoporous carbon supported Pt/MO<sub>2</sub> (M= Ce, Pr, Nd, Sm) heteronanostructure: Promising non-Ru methanol oxidation reaction catalysts for direct methanol fuel cell application," *Journal of Electroanalytical Chemistry*, vol. 794, pp. 86-92, 2017.
- [83] R. A. Hameed, R. Amin, K. El-Khatib, and A. E. Fetohi, "Preparation and characterization of Pt–CeO<sub>2</sub>/C and Pt–TiO<sub>2</sub>/C electrocatalysts with improved



- electrocatalytic activity for methanol oxidation," *Applied Surface Science*, vol. 367, pp. 382-390, 2016.
- [84] R. Amin, R. A. Hameed, K. El-Khatib, M. E. Youssef, and A. Elzatahry, "Pt–NiO/C anode electrocatalysts for direct methanol fuel cells," *Electrochimica Acta*, vol. 59, pp. 499-508, 2012.
- [85] X. Tarrús, M. Montiel, E. Vallés, and E. Gómez, "Electrocatalytic oxidation of methanol on CoNi electrodeposited materials," *International Journal of Hydrogen Energy*, vol. 39, pp. 6705-6713, 2014.
- [86] I. Danaee, M. Jafarian, F. Forouzandeh, F. Gobal, and M. Mahjani, "Electrocatalytic oxidation of methanol on Ni and NiCu alloy modified glassy carbon electrode," *International Journal of Hydrogen Energy*, vol. 33, pp. 4367-4376, 2008.
- [87] M. Kübler, T. Jurzinsky, D. Ziegenbalg, and C. Cremers, "Methanol oxidation reaction on core-shell structured Ruthenium-Palladium nanoparticles: Relationship between structure and electrochemical behavior," *Journal of Power Sources*, vol. 375, pp. 320-334, 2018.
- [88] A. Thakur, S. Kumar, and V. Rangra, "Synthesis of reduced graphene oxide (rGO) via chemical reduction," in *AIP Conference Proceedings*, 2015, p. 080032.
- [89] S. Tkachev, E. Y. Buslaeva, A. Naumkin, S. Kotova, I. Laure, and S. Gubin, "Reduced graphene oxide," *Inorganic Materials*, vol. 48, pp. 796-802, 2012.
- [90] G. Jiang, T. Wu, S.-T. Zheng, X. Zhao, Q. Lin, X. Bu, *et al.*, "A nine-connected mixed-ligand nickel-organic framework and its gas sorption properties," *Crystal Growth & Design*, vol. 11, pp. 3713-3716, 2011.
- [91] A. Kumar, A. Saxena, A. De, R. Shankar, and S. Mozumdar, "Controlled synthesis of size-tunable nickel and nickel oxide nanoparticles using water-in-oil microemulsions," *Advances in Natural Sciences: Nanoscience and Nanotechnology*, vol. 4, p. 025009, 2013.
- [92] D. Zhu, C. Guo, J. Liu, L. Wang, Y. Du, and S.-Z. Qiao, "Two-dimensional metal–organic frameworks with high oxidation states for efficient electrocatalytic urea oxidation," *Chemical Communications*, vol. 53, pp. 10906-10909, 2017.

- [93] W. Hua, Y. Fu, J. Su, S. Yang, G. Li, F. Liao, *et al.*, "Synthesis, structure and magnetic property of a new nickel (II) 1, 4-benzenedicarboxylate," *Journal of Molecular Structure*, vol. 1010, pp. 184-189, 2012.
- [94] B. F. Machado and P. Serp, "Graphene-based materials for catalysis," *Catalysis Science & Technology*, vol. 2, pp. 54-75, 2012.
- [95] E. Antolini, J. R. Salgado, and E. R. Gonzalez, "The methanol oxidation reaction on platinum alloys with the first row transition metals: the case of Pt–Co and–Ni alloy electrocatalysts for DMFCs: a short review," *Applied Catalysis B: Environmental*, vol. 63, pp. 137-149, 2006.
- [96] N. Cao and Y. Zhang, "Study of reduced graphene oxide preparation by Hummers' method and related characterization," *Journal of Nanomaterials*, vol. 2015, p. 2, 2015.
- [97] X. Zhang, Z. H. Jiang, Z. P. Yao, Y. Song, and Z. D. Wu, "Effects of scan rate on the potentiodynamic polarization curve obtained to determine the Tafel slopes and corrosion current density," *Corrosion Science*, vol. 51, pp. 581-587, 2009.
- [98] F. Seland, R. Tunold, and D. A. Harrington, "Impedance study of methanol oxidation on platinum electrodes," *Electrochimica Acta*, vol. 51, pp. 3827-3840, 2006.
- [99] C. Cordeiro, M. De Vries, T. Cremers, and B. Westerink, "The role of surface availability in membrane-induced selectivity for amperometric enzyme-based biosensors," *Sensors and Actuators B: Chemical*, vol. 223, pp. 679-688, 2016.
- [100] G. Behmenyar and A. N. Akın, "Investigation of carbon supported Pd–Cu nanoparticles as anode catalysts for direct borohydride fuel cell," *Journal of Power Sources*, vol. 249, pp. 239-246, 2014.
- [101] W. Huang, H. Wang, J. Zhou, J. Wang, P. N. Duchesne, D. Muir, *et al.*, "Highly active and durable methanol oxidation electrocatalyst based on the synergy of platinum–nickel hydroxide–graphene," *Nature communications*, vol. 6, p. 10035, 2015.
- [102] E. Sarwar, T. Noor, N. Iqbal, Y. Mehmood, S. Ahmed, and R. Mehek, "Effect of Co-Ni Ratio in Graphene Based Bimetallic Electro-catalyst for Methanol Oxidation," *Fuel Cells*, vol. 18, pp. 189-194, 2018.

- [103] Y. Noh, Y. Kim, S. Lee, E. J. Lim, J. G. Kim, S. M. Choi, *et al.*, "Exploring the effects of the size of reduced graphene oxide nanosheets for Pt-catalyzed electrode reactions," *Nanoscale*, vol. 7, pp. 9438-9442, 2015.
- [104] W. Wang, Q. Chu, Y. Zhang, W. Zhu, X. Wang, and X. Liu, "Nickel foam supported mesoporous NiCo<sub>2</sub>O<sub>4</sub> arrays with excellent methanol electro-oxidation performance," *New Journal of Chemistry*, vol. 39, pp. 6491-6497, 2015.
- [105] N. R. Mathe, M. R. Scriba, R. S. Rikhotso, and N. J. Coville, "Microwave-irradiation polyol synthesis of PVP-protected Pt–Ni electrocatalysts for methanol oxidation reaction," *Electrocatalysis*, vol. 9, pp. 388-399, 2018.
- [106] T.-H. Ko, K. Devarayan, M.-K. Seo, H.-Y. Kim, and B.-S. Kim, "Facile Synthesis of Core/Shell-like NiCo<sub>2</sub>O<sub>4</sub>-Decorated MWCNTs and its Excellent Electrocatalytic Activity for Methanol Oxidation," *Scientific reports*, vol. 6, p. 20313, 2016.
- [107] S. Mahapatra and J. Datta, "Characterization of Pt-Pd/C electrocatalyst for methanol oxidation in alkaline medium," *International Journal of Electrochemistry*, vol. 2011, 2011.